Integration Properties of Kenyon Cells in the *Drosophila melanogaster* Mushroom Bodies

A Dissertation Presented

by

Eyal Gruntman

to

The Watson School of Biological Sciences

in Partial Fulfillment of the Requirements

for the Degree of

Doctor of Philosophy

in

the Biological Sciences

at Cold Spring Harbor Laboratory

June 2012

SMELL,

The final frontier. These are the enterprises of a Jewish graduate student. His five-year mission: to explore strange new facts, to seek out new data and new techniques, to boldly go where no man has gone before.

Acknowledgements

No thesis is an island. Although I performed all the experiments in this thesis myself, I could not have done it without the help and support of my friends and colleagues in CSHL. Naturally, I am indebted to my advisor Glenn, for his support when I went through rough times, guidance when I was lost, and patience when I nagged with basic questions. All the Turner lab members were also instrumental with help on different facets of the thesis. Rob Campbell build the odor delivery system and pioneered the 2-photon imaging in the lab, Kyle Honegger helped in designing the MARCM crosses, and Toshihide Hige initiated me into the occult world of whole-cell recordings. I would also like to thank all the members of the 'fly floor' from the Zhong and Dubnau labs, who were all part of a supportive, stimulating and fun working environment. In addition, I would like to thank my committee members, Stephen Shea, Tony Zador, Yi Zhong, and Josh Dubnau who helped me stay on track and provided new perspectives. Finally I would like to thank my family. My parents, for their unvarying encouragement, even though they wished I would opt for a more lucrative profession. And my wife and kids, without whom I would have probably finished the thesis a year earlier - thanks for reminding me there are more important things in life.

Table of Contents

1 Introduction

1.1 Combinatorial Coding in the Brain

When an organism interacts with its environment, it does not look for information – it looks for meaning. As any scientist who received data from a Solexa run can attest, data is easy to come by, but extracting meaning is a challenge. The brain extracts meaning by constructing objects from the deluge of information it is constantly receiving. By making assumptions about the world (some innate and some acquired) the brain is able to extract complex features and detect patterns. It does so by integrating information across different input channels. Each single neuron receives input, integrates it, and has to "decide" whether to fire or not. We have decided to study exactly that process of integration in the fly. Since the neurons we are studying are in a well-characterized system, and they have relatively few inputs, we hoped to gain insight into the decision making process of neurons.

1.1.1 Where the Brain Guesses Wrong

Please take a moment and listen to the short example from Pressnitzer et al. 2011 listed as sound example 7 (http://audition.ens.fr/dp/Frontiers_Sound_Examples/). The piece is Suite no. 3 in G major from suites for solo cello by Johan Sebastian Bach. The reason I have chosen to start my thesis with it is because I believe it epitomizes what the brain does. As can be deduced from the name, there is a single cello playing in this piece. However, we can clearly hear more. As explained in Pressnitzer et al. 2011, the reason for that is the intricate play between the frequency and the time interval between the notes.

When we listen to stimuli from our surroundings, the only input channel is the vibrating membrane in our ear. To deduce from those vibrations how many different sources generate them is an algorithmically ill-posed problem. The brain has to make assumptions about certain frequencies being generated together and about a certain level of constancy through time to solve this problem. The important aspect for our purpose is not so much how the brain solves this problem but that the brain is trying to solve it. When we hear this piece, we are not content with simply registering the vibrations as they come. We imbue them with meaning as to the different possible sources that generate them. We make separate objects out of a continuous stream based on what we assume about the world. But is the ear simply a special case, where the shape of the input imposes implicit solutions? We shall now turn to another example, this time from vision.

1.1.2 Seeing is Believing

There are myriads of visual illusions that shed light onto how our brain works. The reason I chose this one as an example is that when we look at the image displayed in Figure 1.1 our brain seems to be doing a similar thing to what it did when we listened to the cello suite. We perceive two continuous lines that merge behind the rectangle, since our brain is again making assumptions about the world. Even though we can clearly see the two lines do not overlap, we group them into a single object, since most of the clues point us in that direction (same color, same orientation, same spatial contingency). Again we see that our brain is not pleased with simply registering input – it is creating objects.

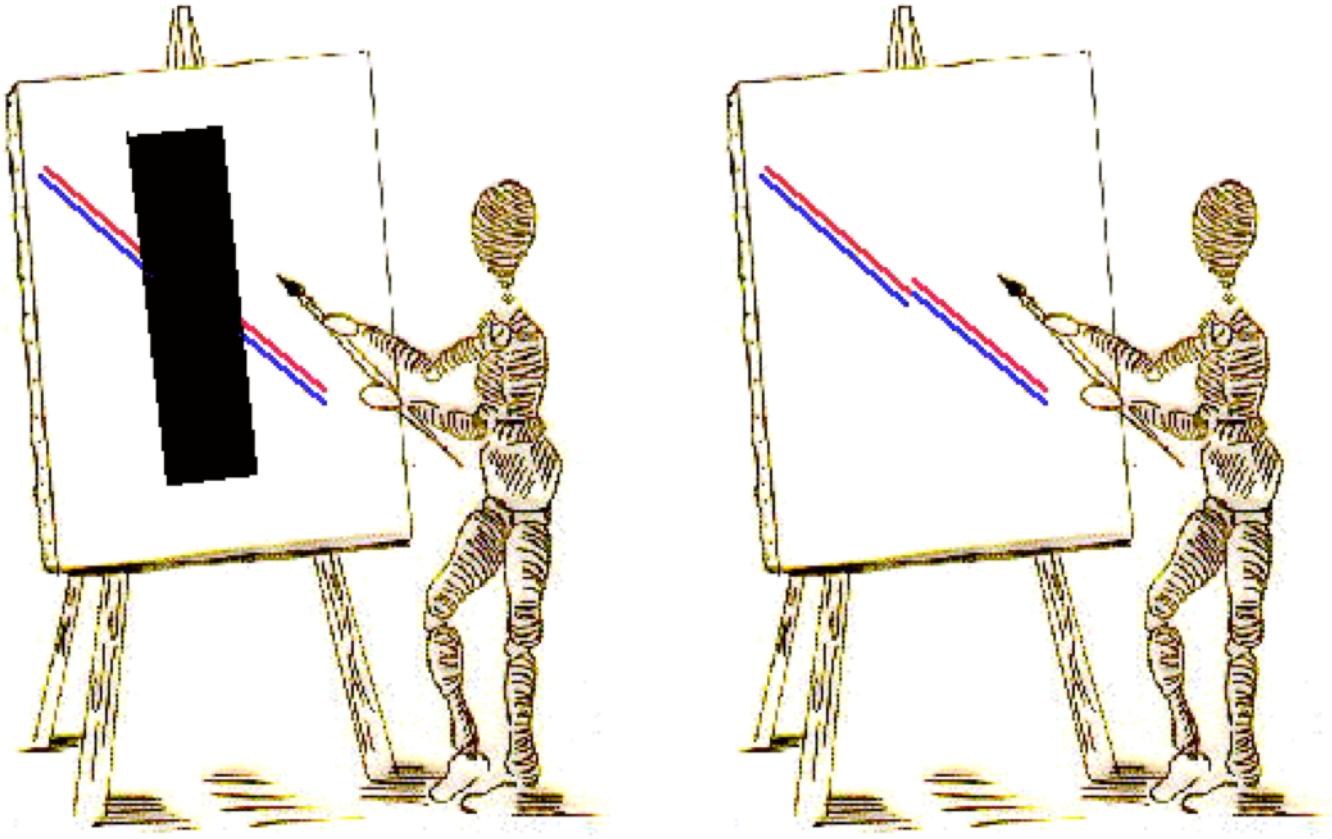

Figure 1.1 Poggendoff illusion. Example taken from UML psychology website (http://dragon.uml.edu/psych/). See text for details.

Lastly, we turn to a different visual example that, hopefully, will convey a slightly different perspective about the workings of our mind. Please flip back and forth between the 2 images in Figure 2 and try to spot the difference between them (example taken from http://www.cogsci.uci.edu/~ddhoff/cb.html, where the illusion can be viewed more easily). If this problem was given to a computer, the solution would be instantaneous. By simply comparing pixel values throughout the image the difference can be clearly spotted. But this is not the way we perceive the image. Again, our brain is not content with simply registering the image – it imbues it with meaning. We perceive depth in the image, we construct objects, and we group them together based on physical proximity and continuity. The few pixels that do not overlap between the images are meaningless to our brain and are therefore not registered. Interestingly, once we perceive the change (a flower in the bottom right corner) we cannot un-perceive it. It becomes blazingly obvious. This tells us another thing about the way our brain works – though it is preprogrammed to look for certain types of meaning (constructing objects) we can actively imbue meaning onto previously ignored parts.

Figure 1.2 Part 1

Figure 1.2 Part 2

1.1.3 The Effort After Meaning

In the transcript from a lecture given in 1984, Horace Barlow repeats a phrase he recalls had influenced him very early on in his career – "the effort after meaning" (Barlow 1985b). The phrase was used repeatedly by his psychology professor, sir Frederick Bartlett, and encouraged Barlow to choose physiology over psychology, since this is where the effort might bear fruit. But what does it mean?

At the same lecture, when Barlow is trying to explain the meaning of the phrase he claims: "… the eye was not so much a detector of light as a detector of patterns created by those objects and events in the environment that were important for the animal (Barlow 1985b)." In other words, as I hope to have demonstrated from the above illusions, stimuli themselves are meaningless. The organism is not interested in sensing them or representing them reliably. It is what the stimuli represent that has meaning to the organism; they are signs to events in the world that are crucial for its survival.

The Estonian physiologist, Jakob von-Uexkull, went so far as to claim that this is what defines biology - the existence of a subject (Uexkull 1982). The subject constructs its own inner world - termed Umwelt - from the cues it extracts from the environment. In this view "Behaviors are not mere tropisms, but they consist of perception and operation; they are not mechanically regulated, but meaningfully organized (Uexkull 1982)."

Again we see that meaning is an organizing principal in biology, and it is ultimately what the organism is searching for in the world (not in an existential sense but in a more concrete one). Therefore, "the effort after meaning" would be our attempt to bridge the gap between the stimuli we present and what the animal perceives. But how can the brain extract meaning from stimuli, and how can we, as researchers, uncover it? A prime example of an answer to both of these questions can be found in the classic work that has been done on visual processing of information. And this is what we shall discuss next.

1.2 The Search for Meaning in the Eye

When physiologists started to record activity in the frog's retina it was obvious that a high level of integration is imperative. The frog's retina has many more photoreceptors than Retinal Ganglion Cells (RGCs), whose efferents are the nerve fibers exiting the eye. It was originally assumed that an individual neuron is noisy and unreliable (Barlow 1972), so it seemed almost natural that only by averaging several inputs can one produce a good image. However, the discovery of on-off units (known today as RGCs with center-surround inhibition) challenged this simplistic view (Barlow 1953). RGCs in the frog retina that have this type of receptive field are not simply averaging inputs; they are not just transmitting information reliably from one level to the next; they are, in fact, extracting features.

Barlow, in his original paper, went so far as referring to these cells as "bug detectors" (Barlow 1953). Although there is no simple relationship between activity in these neurons and food-seeking behavior directed towards the respective receptive fields, the cells do seem to signal something stronger than a trivial change in luminance. In later papers, Barlow refers to what these cells might signify as "trigger features" (Barlow 1972). In that respect, "… an RGC signals that something specific is happening in front of the eye. Light is the agent by which it does it, but the detailed pattern of light carries the information (Barlow 1972)." We can see that even at this level, only 2-3 synapses from the receptors, features are extracted that are meaningful for the animal. Therefore, the retina does not transmit a map of the world, but a map of "trigger features" that were induced by the world (Barlow 1972).

Another conclusion that stemmed from the 1953 study and other studies of the time was that individual neurons were actually reliable. And their reliability was not a result of averaging, but simply of their inherent properties (Barlow 1972). This has led Barlow to suggest a framework in

which the activity of a single neuron can be viewed as a result of an hypothesis test (Barlow 1985a). A neuron with its pattern of synaptic connections and their weights represents a hypothesis about the sense organs it connects to. Its firing indicates how strongly this hypothesis is violated based on the current condition of the sense organs. In that sense, an ON cell tests the hypothesis: "there has not been a local increase in illumination in my part of the retinal image (Barlow 1985a)." We can view these neurons as making up the elementary units of a percept, the units with which we, and other organisms, confer meaning onto the world.

1.2.1 How to Compress Information

We have mentioned earlier that the eye has more inputs than outputs. This implies that the eye is compressing the information it is receiving – but how? This question has gained significant momentum with the advent of information theory into neuroscience, and specifically into vision research (Attneave 1954). Early researchers noticed that natural images are highly redundant in information. Since our visual scene is constructed out of objects, and parts of an object are more similar to each other than they are to the surroundings, parts of the visual scene are highly correlated and so - redundant. A different way of defining this simple feature is that in a natural image information is concentrated where a subject would guess wrong (Attneave 1954). Given knowledge of the proximal part of the image, or even just the sequence of preceding pixels, a subject would be wrong in guessing what the next pixel is where boundaries occur. And if the boundary is regular enough, the subject would guess wrong when the boundary changes orientation, and so on.

Though this approach was exceptionally fruitful, it focused on the information content of the stimulus and not the meaningful information for the organism. Invoking the digital analogy again, if a computer needs to transmit information efficiently, eliminating redundancy is a prime concern. But for the brain transmission is not the main concern - meaning is. Therefore, a more current view of

redundancy treats it not as something to be eliminated but as something to be recognized and exploited (Barlow 2001). And for that we need the cortex.

Signals from the retina are transmitted through the lateral geniculate nucleus to the visual cortex. If we try and attribute a general role for the cortex as such it would be of forming associations. The cortex, according to Barlow, is a gifted detective – looking for suspicious coincidences in the afferent inputs (Barlow 1985a). Coincidences that are unlikely to occur by chance, but not so unlikely as to never occur at all; in other words, coincidences that result from objects in the natural world (Phillips et al. 1984).

As we have already mentioned, the high correlations in the visual input stem from the presence of objects in the natural world. Therefore, redundancy is far from being unnecessary or wasteful, it is indicative of meaningful coincidences that the animal can exploit. The visual system is built so that it can detect those coincidences (Barlow 2001). Support for this view comes from studies that found high correlations between independent components in natural images, and the receptive fields of cells in the visual cortex (e.g. Hateren and Schaaf 1998). To understand more clearly how these coincidences are detected, we will now turn our attention towards the cortex and the computations it performs.

1.2.2 Ceci N'est Pas Une Pomme

In their search for meaning, neuroscientists went deeper and deeper into the brain. The first region in which a significant transformation of the input was found is the striate cortex. Hubel and Wiesel recorded from the cat striate cortex and found receptive fields of two types: simple and complex. The simple cells' receptive fields seem like an agglomeration of receptive fields from the earlier layers (Figure 1.3). By aligning several center-surround receptive fields on a single axis, both orientation-selectivity and increased selectivity to stimuli are accomplished. Complex cells, as their name implies, have even more complex receptive fields. These cannot be described simply by

aligning receptive fields from earlier layers; and more importantly their spatial specificity was dramatically reduced (Hubel and Wiesel 1962).

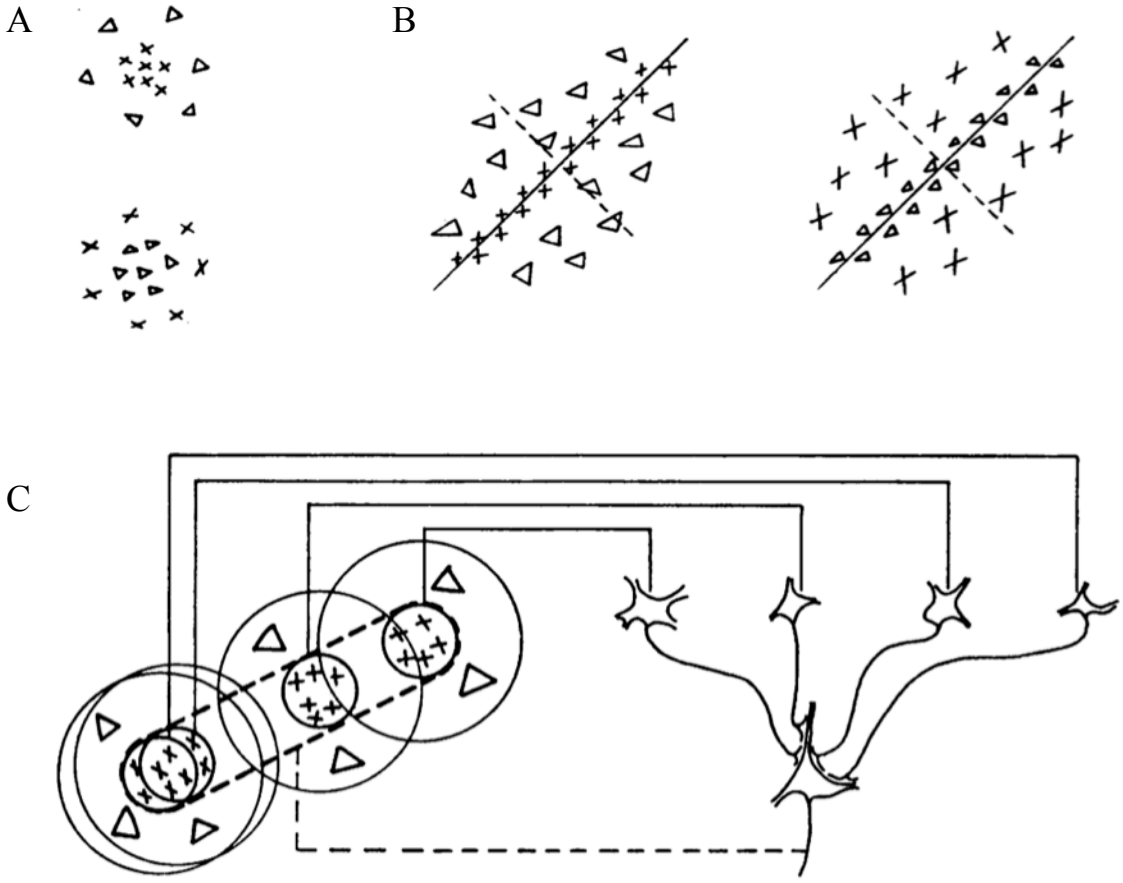

Figure 1.3 Receptive fields in the cat visual cortex **(A)** Example ON (top) and OFF (bottom) cells from the lateral geniculate nucleus. **(B)** Two simple cells receptive fields from the striate cortex. **(C)** A hypothesized model for how the receptive fields in B might be constructed from the more basic receptive fields in A. **X** indicate excitatory responses, and **Δ** indicate inhibitory responses. Images were adapted from Hubel and Wiesel 1962.

Though at this layer we still do not have a firm handle on meaning, we might have a handle on its alphabet. Barlow suggested that the hierarchy in the complexity of receptive fields along the visual pathway might be viewed as the hierarchy in language (Barlow 1985b). First, we have the individual components that make up all the letters - small lines, ticks, and curves. Next, with those components we can construct each individual letter in our alphabet. With the letters we can construct each word and, with the words sentences, and so on (Barlow 1985b). Conceptually, it is easy to imagine how receptive fields of retinal ganglion cells are the building blocks of simple cells' receptive fields (Figure 1.3C). By aligning several basic units together, one might define an edge or another important feature in an image. The appealing nature of the analogy stems, in part, from the realization that a single word, though very specific, still has a wide semantic field and depends upon its context for an exact interpretation. Much in the same way, a single "visual word", be it an edge or a boundary, depend upon its context for the full interpretation.

In that same classic paper, Hubel and Wiesel describe another important property of cells in the striate cortex – binocularity (Hubel and Wiesel 1962). At this layer in the circuit integration and the extraction of features is no longer limited to the information from a single input channel. Later it was shown that the cells responded maximally when the separation in the two eyes was different (Barlow 1985b). This condition would occur only if the stimulating object is at a certain distance, which is exactly what this transformation extracts.

Climbing even higher into the depth of visual processing we find more and more complex "visual words". While recording from the inferiotemporal cortex in monkeys, and as a result of a hand-waving fit of despair, (Gross et al. 1972) found "hand responding" neurons. The high specificity of the stimulus shape plus the relatively large spatial receptive field of these cells conform with the hierarchical prediction Hubel and Wiesel made in their paper (Hubel and Wiesel 1962). Based on their findings, they deduced that cells in higher regions will respond to bigger regions in the retina but will limit their responses to more specific stimuli.

10 years after the finding of the "hand responding" neurons, "face responding" cells were found in the superior temporal sulcus of an alert monkey (Perrett et al. 1982). Although reports of cells of this type have been made earlier, this was the first study in which a detailed characterization of the cells have been made. Surprisingly, the cells responded mainly to frontal views of the face. A sideways turn, even of 5-10 degrees, eliminated the response completely (Perrett et al. 1982). Though it is still not clear how a face responding neuron is made and what are the actual inputs it receives, it is possible to image how it is built with the simple "visual alphabet" that constructs more complex features as we move deeper into the brain.

1.3 The Brain – What is it Good For?

As I hope to have demonstrated, starting with the auditory illusion and ending with the detailed description of visual processing, the brain looks for meaning in the world. It is not simply collecting stimuli passively and registering them, but actively extracting relevant features from the surrounding world. The details in the visual system serve as a guiding principal: features are extracted, at least in part, by integrating nonlinearly over more basic inputs. Each neuron can be regarded as making a statistical statement about the correspondence between its "trigger feature" and the current state of the world (as shown to it by its inputs). By combining such units of higher and higher complexity we can imagine how the brain is able to extract common features. The level at which a specific feature is extracted depends on the organism. What happens at the frog's retina happens in the cat only after three more synapses - but the mechanism is the same (see also Gollisch and Meister 2010 for a recent review of the computation in the mammalian retina).

The same principles apply if we look at different modalities or different organisms. The similarities between the mammalian and the insect visual system, which were already noticed by Cajal (Sanes and Zipursky 2010), allows for a similar investigation with all the advantages of using a

powerful genetic organism. The inputs to the system are fewer, the genetic control of cell types is greater, and accessibility to higher brain regions is usually not an obstacle. A recent study, for instance, found a looming responding neuron in the fly and was able to elicit an appropriate behavioral response in a blind fly by artificially activating that neuron (de Vries and Clandinin 2012).

In what follows I will try to explain why we have chosen to study integration in the *Drosophila* olfactory system, what we already know about the system, and what can we hope to learn from it about the workings of the brain.

2 *Drosophila* Olfactory System as a Model for Combinatorial Coding

2.1 Intrinsically Combinatorial Nature of Olfaction

Odors are an unusual set of stimuli. Unlike light or sound, which are immutable physical entities, odors are generated by other organisms and are therefore constantly changing (both on a phylogenetic and an ontogenetic timescale) (Bargmann 2006). The indication for just how different they are can be found in the outlandish number of receptors that are involved in detecting them. Olfactory receptor (OR) genes are among the largest gene families known, and in the extreme case of rats they comprise about 6% of the functional genes in the genome (Ache and Young 2005).

As the number of odorant receptors suggests, there is no clear dimension across which the odorant stimuli change. If there was one (or even several dimensions for that matter), organisms would likely not need so many different receptors. From the extremely low level of conservation between odorant genes we can deduce that odorant receptors are not ligand-specific. From their appearance in duplicated clusters throughout the genome, we can deduce that they are probably also not independent. They are changing as part of the response to the constantly changing environment (for a recent example see McGrath et al. 2011). As such, they are probably not specific detectors of features, but fuzzy detectors that add just enough information to be preserved through evolution.

Indeed, as the genetic data on ORs predicts, the responses of Olfactory Receptor Neurons (ORNs) are inherently combinatorial. In a tour-de-force experiment (Hallem and Carlson 2006) have characterized the response of more than half of the ORNs in *Drosophila* to a set of 110 odorants. A clear outcome of the study was that every odor elicited a response in several ORNs; and every ORN

was activated by several odorants (Hallem and Carlson 2006)(apart from a few labeled line examples that will be discussed later). This leads us to the inevitable conclusion that for a fly to identify an odor uniquely, inputs from different ORNs need to be integrated. The above principle is true for most organisms, from nematodes to humans (Ache and Young 2005). In the next section we will discuss the anatomy of the fly's olfactory system and try to deduce the possible site for such integration.

2.2 Mushroom Bodies Are the Main Sites for Olfactory Integration

In this section I describe the evidence we had pointing to the Kenyon Cells (KCs) of the mushroom bodies as the main sites of integration along the olfactory circuit. The evidence is from both anatomical and functional studies. However, before we delve into the details, I will provide a brief description of the olfactory circuit of the fly.

2.2.1 How Do Flies Smell?

A lot has been learned about the fly olfactory system, from the different receptors that are expressed in each type of sensilla, to the different odorant binding proteins that facilitate olfactory perception (for a detailed review see Laissue and Vosshall 2008). For the purpose of my thesis, our main focus will be the connectivity pattern within the circuit, since it implies where integration of the different olfactory channels might occur.

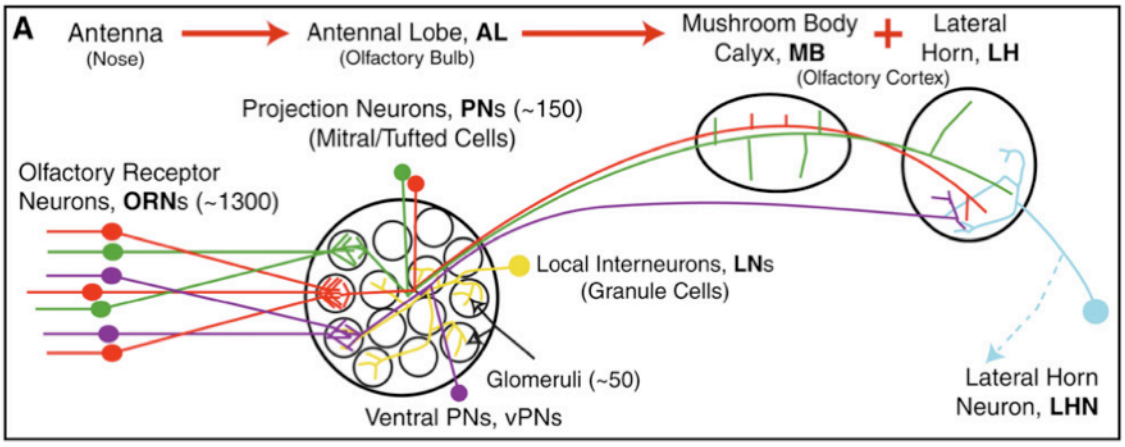

Figure 2.1 Schematic of the fly olfactory circuit. See text for details. Image taken from Jefferis 2007 Cell.

The first layer of the olfactory system in the fly is comprised of the Olfactory Receptor Neurons. Most ORNs express a single OR, in addition to co-receptor Or83b (Sato et al. 2008). All the ORNs that express the same receptor project to the same region in the Antennal Lobe called a glomerulus (see Figure 2.1) (Vosshall et al. 2000; Fishilevich and Vosshall 2005). In the antennal lobe, each glomerulus is innervated by several Projection Neurons (PNs). The antennal lobe also has several different types of Local Interneurons (LNs) that innervate numerous glomeruli, but we will discuss their function in section 2.2.3.2 . PNs that innervate the same glomerulus are considered to constitute a single PN type, since both their projection patterns and their spiking patterns are highly correlated (see below). For that reason, the olfactory system in *Drosophila* is usually regarded as having ~54 different input channels (the number of different glomeruli). Though still a substantial number when considering combinatorial activation patterns, it is far less than other commonly studied insects, or mammals.

From the antennal lobe, PNs project to higher brain regions in the fly, which are called the mushroom bodies and the lateral horn. The lateral horn in *Drosophila* is considered to be responsible for innate olfactory behavior (e.g. Suh et al. 2004; Jefferis et al. 2007) and will only be discussed in this work in reference to the mushroom bodies. PN projections into the mushroom bodies form relatively large synaptic boutons (5-6μm) in a region called the mushroom body calyx. The boutons are innervated by the intrinsic cells of the mushroom bodies – the Kenyon Cells. The KCs send their axons in bundles to output regions named the mushroom body lobes, and these contact a diverse group of extrinsic neurons. There are several PNs that innervate multiple glomeruli, but those are far fewer than the 'typical' uniglomerular PNs, and they mostly bypass the calyx (Tanaka et al. 2008; Okada et al. 2009).

2.2.2 Integration in Kenyon Cells– Anatomical Evidence

Golgi impregnations of individual KCs in the fly revealed that these neurons form unique dendritic structures in the calyx (Strausfeld et al. 2003). The structures were described as claws, wreaths, clusters, or rosettes, but they all were comparable in size and matched PN bouton size. Later studies using 3-dimensional electron microscopy reconstructions have confirmed that PN boutons are in fact contacting KC claws (Leiss et al. 2009; Butcher et al. 2012). Furthermore, it has been shown that several KCs can contact a single bouton (Leiss et al. 2009), and that PNs are the main source of input to the KCs (Butcher et al. 2012). What remains undetermined is whether a single KC actually contacts several different PN types or just a single input channel.

Another line of evidence that suggests KCs can integrate inputs comes from the study of PN projection patterns into higher brain regions. As mentioned above, PN dendrites in the antennal lobe are well organized and constrained within glomeruli. PN projections to the lateral horn, though less constrained, are still organized into regions. This is especially true for PNs that convey fruit odors versus PN that convey conspecific odors (Jefferis et al. 2007). Projections to the mushroom bodies, on the other hand, are considerably more intermingled (Marin et al. 2002; Jefferis et al. 2007; Lin et al. 2007). Though it is still possible to identify a PN type based on its projections (Lin et al. 2007), the arborization zones of different PN types in the calyx are much more overlapping than in the lateral horn. This divergent anatomical organization implies the mushroom body calyx is an integrative region.

2.2.3 Integration in Kenyon Cells – Functional Evidence

2.2.3.1 PNs Type as Single Input Channels

Previously I stated that we can regard all the PNs that innervate a single glomerulus as a single type. The support for this claim is both anatomical and functional. As mentioned in the previous paragraph, projections to higher regions from the same PN type are highly similar between

different brains (Marin et al. 2002; Jefferis et al. 2007; Lin et al. 2007). Though some of the studies disagree as to the degree of similarity in the mushroom body calyx (Jefferis et al. 2007; Lin et al. 2007), it is clear that projections in the lateral horn are stereotyped, and imply similarity of inputs.

To address the similarity between PNs from the same type from the functional perspective (Kazama and Wilson 2009) performed dual recordings from homotypic PNs (from the same glomerulus). They have found that homotypic PNs are highly correlated, both in their sub-threshold activity and in their odor-evoked activity (Kazama and Wilson 2009). The correlations originated from the PN layer, since no correlations were found between ORNs from the same type. The dendritic arbor of a PN innervates the entire glomerulus (Kazama and Wilson 2008), and in fact all the PNs of one type connect to all the ORNs projecting to that glomerulus. Therefore, they receive exactly the same input, and can be regarded as multiple copies of the same channel.

2.2.3.2 Integration in the Antennal Lobe Functions Mainly as Gain Control

Though the antennal lobe contains both multiglomerular PNs and LNs, they are not considered to play a major role in integrating information across input channels. The multiglomerular PNs are the minority among the PNs and most of them bypass the calyx and project directly to the lateral horn (Tanaka et al. 2008). Though it is possible they play a role in integrating channels that elicit innate responses to odors, they are not considered to play a major role in acquired odor preferences.

The LNs in the antennal lobe are also known to contact multiple glomeruli. However, recent studies have shown that LNs are mostly GABAergic and that their main function is to apply a gain control mechanism in the antennal lobe (Olsen and Wilson 2008; Olsen et al. 2010). Tracing individual LNs has shown that most of the neurons arborize to almost 90% of the antennal lobe, making specific integration a minor component of the layer (Okada et al. 2009; Chou et al. 2010). Additionally, by isolating direct and indirect inputs to PNs, Olsen et al. (2010) were able to show that the LN circuit boosts weak PN responses while attenuating strong responses, so as to increase the

dynamic range of the PNs. No specific integration across input channels was found (Olsen et al. 2010). Although a modeling study has predicted a role for lateral inhibition also in decorrelating PN inputs, this is still achieved by global and not by specific integration (Luo et al. 2010). Note however, that it has also been shown that the coincident-detector *Rutabaga* is required in the PN for appetitive memory to form (Thum et al. 2007).

2.2.3.3 Functional Integration in Kenyon Cells

For years it has been well-established that the mushroom bodies are necessary for olfactory learning and memory. Studies that either ablated the mushroom bodies specifically (de Belle and Heisenberg 1994), or disrupted their activity during different phases of memory (Dubnau et al. 2001; Schwaerzel et al. 2003; Krashes et al. 2007) have shown that these regions are necessary for acquired odor behaviors, but not innate odor preferences (see for example Suh et al. 2004). The flies in these studies still avoided the odors and the shock to a similar extent as wild type flies, which suggests that they did sense the odors, but they did not form any association. Forming a specific odor memory requires the full odor percept, which will require the integration across input PN channels.

Additionally, we know from KC recordings that odor responses in this layer are sparser when compared to the PN layer, both in terms of the number of spikes evoked and the number of odors that evoke a response (Turner et al. 2008). In fact, a recent study from our lab has shown that sparseness is an underlying characteristic of the mushroom bodies (Honegger et al. 2011). As described in the introduction, sparse responses are usually indicative of higher integrative brain regions. If we return to Barlow's model, a sparse and strong response is indicative that a significant meaningful event has occurred, and meaning can only be detected by integration.

2.3 Of Mice and Flies

Evidence for integration of PN inputs can also be found from a comparison to the mammalian olfactory system. Surprisingly, the architecture of the *Drosophila* olfactory system is similar to that of mammals (for reviews see Strausfeld and Hildebrand 1999; Ache and Young 2005; Bargmann 2006). As in flies, sensory neurons express a single OR, and all the neurons that express the same receptor project to a single glomerulus in the olfactory bulb (equivalent to the antennal lobe; see also Figure 2.1). Glomeruli are innervated by Mitral cells that project to higher brain regions like the piriform cortex (PCx) and the amygdala (mammalian equivalent to mushroom bodies and lateral horn, respectively). Naturally, the system is more complex in mammals. Most notably by various different forms of interneurons in the olfactory bulb (for an example on their processing role see (Fantana et al. 2008), and by feedback from the cortex back to the bulb, which so far has not been convincingly shown in flies (but see Hu et al. 2010).

The question of whether third layer neurons (PCx cells) receive convergent input from different glomeruli was also addressed in mammals, and can therefore shed light into our inquiry in flies. A recent anatomical study (Miyamichi et al. 2011) has used retrograde trans-synaptic tracers to label the connections between mitral cells and cortical cells. By counting the number of starter cells labeled in the cortex and the corresponding mitral cells labeled in the bulb, the authors were able to show that the different mitral cells converge onto a single cortical neuron. However, due to the inefficiency of the tracer it cannot be determined what is the exact number of mitral cells that connect to one cortical neuron. Additional tracing studies have shown that PCx projections of homotypic mitral cells are as similar as heterotypic projections, implying a low level of stereotypy (Ghosh et al. 2011; Sosulski et al. 2011).

Functional studies that addressed this question have also found evidence for input integration. (Stettler and Axel 2009) used calcium imaging in the cortex to find PCx cells that respond specifically to mixtures. A synergistic response to the mixture implies convergent input from different mitral cells (Stettler and Axel 2009). Similar results were found when imaging mitral cells presynaptic responses in the PCx, which accounts for intracortical connections (Mitsui et al. 2011). A

more recent study used glutamate uncaging to induce controlled activation of combinations of mitral cells. By recording the evoked responses in cortical cells, they were able to show that third layer neurons respond to specific combinations of inputs (Davison and Ehlers 2011). The responses were clearly supra-linear, implying that combinations of inputs are much more efficient at driving PCx cells.

2.4 On Odor Objects and Their Creation

We shall now take a brief hiatus from experimental evidence and return to a theoretical discussion. As you may recall, in the introduction we emphasized the role object construction plays in the extraction of meaning. Auditory objects are the independent sound sources detected in a stream; visual objects are ontological entities detected by edges and their orientations; but what is an olfactory object? And, more importantly, what is an olfactory object for a fly?

An attempt to answer the first question was given in a recent review (Gottfried 2010). Gottfried sees the odor object as possessing similar qualities to that of a visual object. (1) *Feature synthesis* – an object is made up from several components that create a single percept. For a visual object the features are edges and colors; for an odor object they are the components of a mixture. (2) *Figure-ground segmentation* – an object can be separated from its background. For a visual object it is the ability to distinguish it from its surroundings; for an odor object it is the ability to detect it over a background odor. (3) *Categorization* – the ability to form equivalence groups for objects. For a visual object it could be the ability to group all images of an apple into a group "apple"; for an odor object it would be to group the different aromas of apples into a single group. (4) *Separation* – the ability to discriminate between similar objects. Continuing with the same example, for a visual object it is the ability to distinguish between Gala and Pink Lady; and for an odor object it would be the ability to distinguish between their aromas. All of these properties have been shown for odor percepts,

both in humans and animals (Gottfried 2010), making the concept of an "odor object" an experimentally useful concept.

Though any perceived object can be regarded as the equivalence group that holds the same meaning, this is especially true for odors. When we smell an apple, even between our first and second whiff of it, the stimulus itself changes. Wind direction, background odors, humidity, temperature, and the discontinuous nature of the odor plume, all affect the actual composition of volatile chemicals. So if an object is in essence a category, creating an object means defining the boundaries of a category and refining them. In humans and rats we know that the boundaries can be very fine, since they can be taught to distinguish between enantiomers (Rubin and Katz 2001; Li et al. 2008). Considering the limited number of inputs entering the fly's olfactory circuit, it seems safe to assume that its odor categories are much broader.

In the mammalian olfactory circuit the assumption is that different regions are responsible for encoding different facets of an odor. As mentioned above, the amygdala is responsible for innate responses, and should therefore have broad odor categories. The PCx encodes quality in its posterior part and identity in its anterior part (Kadohisa and Wilson 2006). Odor categories in the PCx should be finer than the amygdala, and categories in the anterior part should be finer than those in the posterior part. If we now return to the fly's circuit and take into account the small number of cells actually reading the mushroom body output, it is possible that the fly does not encode odor identity at all, but only encodes odor quality (fruity, flowery, minty, etc.).

In this context it is interesting to speculate what do the mushroom bodies actually do in the circuit. We know that the highly specific response properties of KCs are distinctive within the olfactory circuit (Turner et al. 2008). Projection neurons, extrinsic neurons (that contact the mushroom body output), and probably also lateral horn neurons, are all more broadly tuned and respond with many more spikes (Wilson et al. 2004; Gupta and Stopfer 2011) Hige Toshihide personal communication). Based on these responses, I assume that if categorization is performed anywhere in the circuit, it is likely to be performed in the mushroom bodies. As a consequence, the

function of the KCs would be to encode these categories, refine them as a result of experience, and possibly also assign an input to a different category. If this is true, a predicted consequence is that associative learning in flies should induce a more generalized association than an equivalent association in mice, though it is not easily verified experimentally.

This is another theoretical reason for integration to occur at the mushroom bodies. The first synapse of the circuit is one of amplification, with similar ORNs converging onto a single glomerulus. Within the antennal lobe the main processing is of gain control, which accounts for different intensity of the stimulus. If the KC layer is responsible for categorization, as its responses imply, then integration across channels should be a fundamental property of that layer.

2.5 How do Animals Integrate Information?

When we wish to consider how an organism integrates inputs to decide about an appropriate behavior, the simplest possible answer is – it does not! Labeled lines have long been suggested as the mechanism by which animals choose their actions. Since Sherrington's "concatenation of reflexes" (Sherrington 1923) and Barlow's "bug detectors" (Barlow 1953), it was thought that certain inputs act as triggers for certain behaviors in a very direct way. Current examples include studies on the CO_2 sensing glomerulus in *Drosophila*, whose activity alone evokes avoidance behavior (Suh et al. 2004). A similar concept was asserted in (Semmelhack and Wang 2009), who found that activation of certain glomeruli induced either innate avoidance or innate attraction to an odor (Semmelhack and Wang 2009). Similarly, in the gustatory system, it was found that a neuron in the sub-esophageal ganglion, which controlled proboscis extension, seemed to regulate extension by adding up the sweet and bitter inputs (Gordon and Scott 2009). In the latter two examples the response of the fly was seen as tallying the innate values and acting accordingly. However, since the responses are tallied, somewhere in the circuit a neuron needs to integrate inputs and "decide", even in this labeled line scenario.

Recently the labeled line model has been challenged even on its most solid ground – innate behaviors in simple organisms. In *C. elegans* a switch between attraction and repulsion was found to involve just a single olfactory neuron (Tsunozaki et al. 2008). A neuron that was associated with attraction was found to induce repulsion by simply using an alternative mode of neurotransmission, and without invoking any of the known avoidance neurons (Tsunozaki et al. 2008). Work done in pheromone processing in moths has found that even in the macro-glomerular complex coding is still combinatorial and the pheromones of different species are distinguished by the ratios of the components and not their identity (Galizia and Rössler 2010). Studying social recognition in ants, (Brandstaetter and Kleineidam 2011) have shown that odor-cues from nestmates and non-nestmates evoke overlapping response patterns in the antennal lobe (Brandstaetter and Kleineidam 2011). This again suggests that combinatorial processing is integral to even these highly specific innate behaviors.

To cross the chasm between stimulus and behavior we must therefore consider combinatorial coding and integration across different input channels. A recent study from the Konnerth lab, for example, has examined integration in cortical neurons by looking at dendritic hotspots and their distribution along the dendritic tree (Jia et al. 2010). The authors were able to detect individual inputs on the dendritic arbor, characterize them, and deduce that adjacent dendritic segments are tuned to distinct orientations. However, it still seems an insurmountable challenge to deduce how receiving random orientations inputs dispersed along the arbor would produce a specifically tuned neuron. Another study of dendritic integration was focused on the barrel cortex and was therefore able to assess the contribution of individual inputs. By comparing responses to the primary whisker versus the surround whisker, the authors were able to show that some dendritic hot spots respond to both. Although the authors have shown integration within a hotspot, it is still unclear how it relates to the integration performed by the entire dendritic arbor (Varga et al. 2011). Due to the size of pyramidal neurons and the number of synaptic partners these studies can only provide a glimpse into the intricate dynamic network that drives a cortical neuron. And that is why we have chosen to focus on KCs as a model for combinatorial coding.

As mentioned, *Drosophila* KCs have only a few olfactory inputs (between 5-7). The inputs themselves are clearly demarcated by the claw structure, which facilitates online identification for *in-vivo* manipulations. The olfactory system in flies has been very well characterized in its first two layers (Vosshall et al. 2000; Hallem and Carlson 2006; Jefferis et al. 2007), so the inputs to the system and their properties are known. Additionally, the powerful genetic toolbox in flies allows us to manipulate different layers independently and assay the effect on integration output.

2.6 Synopsis

Inputs from individual ORNs converge onto few PNs, and these in turn diverge within the mushroom body calyx. In the next layer, the Kenyon cells display both unique anatomy, with several distinct dendritic claws, and unique functional properties, with sparse and brief responses. It all points to the KCs being the main site for integration of olfactory input channels. It is thought that this type of integration diversifies the available tuning curves in the olfactory system, thus enabling more specific odor responses. But how does a KC integrate? How many different inputs does it actually receive? And how many of them must be active to induce a response? At one extreme is a KC as an obligate integrator that only spikes when all its inputs are firing. This will ensure sparse responses and will generate new and narrower tuning curves than those possessed by PNs. On the other extreme is a KC as an amplifier that receives inputs from identical PN types. This will decrease detection threshold and confer identification of odor specificity to the next layer in the brain. We have decided to test where between these two extremes lie the response properties of KCs. For that purpose we have devised two experiments.

The first experiment was designed to test whether dendritic claws of an individual KC receive different inputs. We used calcium imaging in individual KCs to establish the odor tuning curves of all

the dendritic inputs to the cell. By comparing tuning curves of different claws we conclude that KCs receive different inputs channels.

The second experiment was designed to test how many different inputs must a KC receive and how strong do they need to be, for a KC to spike. We have used a sparsely expressing PN driver to drive Channelrhodopsin-2 (ChR2) in just 3 glomeruli out of the 54. Using whole cell recordings we then establish the functional relationship between the PN subset and a particular KC. Post-hoc imaging allowed us to determine the number of anatomical connections between the recorded cell and the stimulated PNs. Combining the functional and the anatomical results showed that KCs require three active inputs to fire reliably, and that spatial integration across claws is more effective than temporal integration within a claw.

3 Dendritic Tuning Curves Show KCs Receive Different PN Inputs

3.1 Abstract

The experiment described in this chapter was designed to answer one of the open questions in fly olfaction: do KCs integrate inputs from different PN types or do they receive information just from a single type. In other words, do KCs utilize the combinatorial code, forming the odor percept, or do they function as labeled lines, transmitting specific odor channels reliably.

To address this question we chose to characterize the tuning curves of all the PN inputs of an individual KC. We reason that since the inputs coming from the same PN type are highly correlated (Kazama and Wilson 2009), rank order inversions will indicate different inputs converging onto the same cell. By expressing GCaMP3 (Tian et al. 2009) in individual KCs we were able to acquire olfactory responses of KC dendritic sites in a live fly. Comparing the tuning curves of all the inputs from the same cell allowed us to conclude that KCs do receive different inputs. Additionally, we see that those inputs are more correlated than chance, implying a biased sampling of PN inputs.

3.2 Background

As discussed in the Introduction, there are both anatomical and functional reasons that lead us to believe integration of olfactory input is occurring at the KC layer. Functionally, it has been known for quite some time that the mushroom body is involved in olfactory conditioning (de Belle and Heisenberg 1994). Since the region is required for forming a specific olfactory memory (i.e.

associating a particular odor with a particular punishment or reward), it is likely that the odor percept has to form in this layer. Additionally, it is known that KC odor responses themselves are sparse and specific (Turner et al. 2008), which is a hallmark for higher integrative brain regions.

Electron microscopy reconstruction studies (Yusuyama et al. 2002; Leiss et al. 2009; Butcher et al. 2012) have established that the main inputs coming to a KC are through its connections with the PN boutons. Each KC has between 5-7 input sites (Butcher et al. 2012, and our data) with which it contacts the PN boutons in the calyx. Each site is clearly demarcated by a claw shaped structure that is comparable in size to the KC soma (3-4μm) and sometimes even bigger (Strausfeld et al. 2003). This unique anatomy allows us to identify the KCs olfactory input sites online in functional imaging experiments, focus on these regions, and determine their odor response properties.

Our hypothesis is that a single KC receives inputs from several different PN types. To test this we looked for differences in the response properties of dendritic claws belonging to the same cell. There are two experimentally supported assumptions that bridge between this hypothesis and our practical approach: (1) Claws are the main point of contact between PNs and KCs. (2) PN inputs of the same type are highly correlated. Assumption 1 is supported by several studies from the Meinertzhagen lab (Leiss et al. 2009; Butcher et al. 2012), and assumption 2 is supported by studies from the Wilson lab (Kazama and Wilson 2009). For more details on the supporting experiments please refer to sections 2.2.2 and 2.2.3.1, respectively.

These studies provide a basis for us to deduce that different odor response properties in the claws of a KC reflect differences in PN input. Naturally, not any difference in the tuning curve indicates different PN inputs. Differences in magnitude of response across claws or even tuning curves that appear to be thresholded versions of one another could simply arise from technical reasons (e.g. differences in GCaMP levels). Therefore, only rank order inversions in the tuning curves would imply different inputs, and those have been the focus of our analysis.

3.3 Methods

Fly strains

Flies used in this experiment were 2-5 day old females generated from crossing hs-FLP, tubP-Gal80, neoFRT(19A); UAS-GCaMP3; myr-tdTomato/TM3, ser to neoFRT; OK107 flies. The first stable line for the cross was generated using Bloomington stock 5133 (hs-FLP, tubP-Gal80, neoFRT(19A); Pin^{yt}/CyO), crossed with UAS-GCaMP3 (courtesy of Loren Looger), and myr-tdTomato (courtesy of Tom Clandinin). The second line was generated from Bloomington stock 1744 and Gal4-OK107 (Connolly et al. 1996). The above cross produced heterozygote flies that were then heat shocked to generate single or double cell clones using the Mosaic Analysis with a Repressible Cell Marker (MARCM) technique (Lee et al. 1999). This allowed us to express the red tdTomato as an anatomical marker, and the green GCaMP3 as a functional indicator in a single KC.

Generating sparsely labeled clones

To generate single cell clones we decided to use the MARCM technique. The technique induces a mitotic recombination between two FRT sites. The event is stochastic and is initiated by expressing Flipase from a heat shock promoter. The recombination releases the Gal4 driver from its Gal80 repression in a clone of cells (for more details see Lee et al. 1999). The following procedure was used to generate the clones.

Mated females were transferred onto an agar plate in the morning and encouraged to lay eggs by supplementing the plate with a dab of yeast paste. After 4 hours the females and the yeast paste were removed, and the plate was placed in a 25°C incubator for 23 hours. The following morning the plate was cleared from all the hatched larvae and placed in the incubator for an additional 2 hours. The newly hatched larvae were then collected into a fresh vial and placed back at 25°C. After an additional 4 days, vials were transferred into a heated water bath and heat-shocked for 20-30min at 37°C. 4 days were selected to increase the probability of labeling α`/β` neurons, which are known to

be more responsive to odors (Turner et al. 2008). 20-30min was selected to increase the probability of generating either a single or a double-labeled clone (dual clones were imaged only when the processes were clearly separated). We have found that by using this protocol we could get a useful clone, on average, every 4 flies (the two brain hemispheres mean that each fly is in fact two separate experiments).

Animal preparation

Flies were anesthetized on ice briefly and inserted into a hole cut in the aluminum foil of the recording platform. The fly's head was tilted forward so as to expose the caudal part, and the fly was glued to the platform using fast drying epoxy (Devcon 5min Epoxy). The position of the fly was such that the antennae were exposed to the air below the recording platform, while the head capsule could be opened and exposed to saline on the upper side of the platform. Sometime it was necessary to glue to proboscis inside its socket. The proboscis retractor muscles (Muscle 16) were removed from between the antenna to minimize brain movement. The head capsule was opened using fine forceps, the air sacks, and fat residues were removed, but care was taken not to remove the peri-neural sheath.

Odor delivery

Chemicals used in the study were: apple-cider vinegar (Richfood), 1-Hexanol (CAS No. 111-27-3), 2-Phenylethanol (60-12-8), Pentyl acetate (628-63-7), Methyl benzoate (93-58-3), trans-2-hexanal (6728-26-3), Geraniol (106-24-1), and 3 essential oils from AuraCacia: Peppermint, Pine and Orange. Odors were presented using a custom-built odor-delivery system at a flow rate of 1liter/min (for more details see Honegger et al. 2011). Odors were delivered at a 1:20 air dilution to increase response probability. Odor pulses were 1sec long and reached the fly with a latency of ~400ms after valve switching (due to the distance between the final valve and the platform). Photoionization detector (PID) traces were recorded for most odor presentation to ensure stimulus reproducibility. Odors were diverted to the PID by a separate tube with an identical length, to recapitulate the latency to the fly.

Calcium imaging

Two-photon imaging was carried out using a Prairie Ultima system (Prairie Technologies) and a Chameleon Ti-Sapphire laser (Chameleon XR, Coherent Inc.) tuned to 920 nm. Laser power was tuned to deliver the minimal amount of power that still allowed detection of the dendritic processes in the red channel (not more than 8mW at the sample). All images were acquired with Olympus water immersion objectives (LUMPlanFl/IR 60x, 0.90 NA). Extracellular saline contained (in mM) 103 NaCl, 3 KCl, 4 MgCl2, 1.5 CaCl2, 26 NaHCO3, 5N-tris(hydroxymethyl) methyl-2-aminoethanesulfonic acid, 1 NaH2 PO4, 10 trehalose, and 5 glucose. Saline osmolarity was adjusted to 275 mOsm with sucrose if necessary and equilibrated to pH 7.3 by constantly bubbling with a mixture of 95% O2 -5% CO2. The preparation was continuously superfused with this solution throughout the recording.

Flies were dissected and placed under the microscope to identify whether they possessed a useful clone (either single cell or 2-cell clone with non-overlapping processes). When such a clone was found a low-resolution z-stack was taken so as to identify all the possible claws of that clone. Claws were then imaged sequentially (claws were imaged simultaneously only when they were exactly on the same image plane) at a frame rate of around 12Hz. If the first 3 dendritic claws of a cell did not display any odor response acquisition was aborted.

Odors were presented at least 3 times in a pseudo-random order using custom built Matlab routines (MathWorks 2010). The inter-stimulus interval was 18s, with a 1s odor pulse delivered 8sec after trial onset. Data were acquired from 4s prior to stimulus delivery until 6s after.

Data analysis

Data were analyzed using custom routines written in Matlab. To correct for motion artifacts we aligned frames from the same trial by calculating a translational-based discrete Fourier analysis (Guizar-Sicairos et al. 2008) on the red channel and applying the translation on both channels. Since each individual frame was too noisy to allow for movement correction, 3 sequential frames were averaged, then median filtered, and the resulting translation was applied to the middle frame. The

same algorithm was then applied again to the mean images of each trial to correct for movement between all the trails from the same claw.

A Region of Interest (ROI) was selected manually for each claw in the frame. The ROI was tailored to the actual image of the claw by identifying the right-most trough in the log-histogram of pixel values (this was based on the observation that ROIs in the 'background' areas of the frame lack the right-most component). Using this algorithm, pixels that lacked signal throughout the presentation were eliminated from the ROI.

To calculate the magnitude of the response the following steps were taken. First, the mean fluorescent (F) signal was calculated for green (GCaMP) and red (tdTomato) channels separately based on the corrected ROI. Second, the red channel was corrected for photo-bleaching by fitting an exponential to the means of red F values of all the trials from the same claw (only the red channel was corrected since it displayed obvious bleaching between trials). Third, frames in which the red signal was 2 standard deviations below the mean for that claw were discarded from the analysis. If a trial had more than 65% of its relevant frames (frames in the baseline and response periods) discarded based on this criterion, the whole trial was discarded. Fourth, a $\Delta F_{Green}/F_{red}$ value was calculated for each frame using this formula: $(F(t)_{Green} - Fb_{Green})/ F(t)_{Red}$. Here F(t) is the fluorescent signal for that frame and Fb is the baseline fluorescence (defined as mean F 3s before the odor delivery valve opens). Finally, the response to the odor is calculated for each ROI by adding $\Delta F_{Green}/F_{red}$ values that were bigger than two standard deviations from the baseline. If no such frames were found the response was defined as zero, and no negative responses were calculated. The calculated responses will be referred to from hereon as $\Delta G/R$.

Tuning curve correlation

To calculate the correlations between different tuning curves we chose the rank based correlation measure Kendall's τ. The built-in Matlab function *corr* was used with the ranks being generated by the *tiedrank* function. The reason we chose this measure was to account, at least partially, for technical thresholding artifacts. The measure itself calculates all the shared ordered pairs

of the 2 rank sequences and subtract all the non-shared ordered pairs. Normalizing by all the possible pairs generates the correlation value (see explanation for Figure 3.5 for more details).

3.4 Results

Flies rely on olfactory cues to find food, mates and oviposition sites, which is probably irrelevant for this thesis. However, flies are also capable of forming associations between novel odors and aversive or appetitive stimuli (Tully and Quinn 1985; Schwaerzel et al. 2003). Since even monomolecular odors evoke responses in several distinct input channels (Hallem et al. 2004; Hallem and Carlson 2006), forming specific associations would require integration across said channels. We have decided to focus on KCs as the likely site of integration for several reasons. First, earlier layers do not show any local integration. Although LNs do contact several glomeruli, they usually cover the entire antennal lobe and mainly provide global gain control (Kazama and Wilson 2009; Okada et al. 2009). Second, the unique anatomical structure of KC dendrites implies integration. KCs have large claw-like dendritic structures that have been shown to contact large PN boutons (Leiss et al. 2009). Yet, It is still unclear whether they actually contact different PN types. Third, KCs unique response properties imply integration. Both neurons of deeper layers and neurons of more superficial layers show odor responses that are more broadly tuned. KCs sparse and specific responses (Turner et al. 2008; Honegger et al. 2011) are indicative of higher integrative brain regions.

To reveal whether KCs are the actual site of olfactory integration we chose to characterize odor-tuning curves of individual dendritic inputs from the same cell. For that purpose we have expressed the genetically encoded Ca^{+2} indicator, GCaMP3, in individual KCs and assayed their olfactory responses throughout the dendritic tree.

3.4.1 KC Dendritic Claws Generate Distinct Responses to Odors

To assay odor responses from all the dendritic claws of a neuron, we have optimized conditions to both increase the probability of sparsely labeled clones and increase the probability of seeing a response. Since the clones analyzed in this study were generated using the MARCM technique (Lee et al. 1999), it was necessary to adjust the duration of the heat-shock so as to produce single cell clones, and to determine the heat-shock timing so the clones would be from the α`/β` population (see Methods). We chose to focus on single cells, since it removed the need to trace neurites and assign individual claws to a neuron. And we focused on the α`/β` population to increase the probability of seeing an odor response (Turner et al. 2008). Figure 3.1A shows the distribution of cell types in this study, and it is clearly biased towards the α`/β` population. However, since we could not find any obvious difference between the types, for the purpose of our analysis we have grouped all the cells and treated them as a single population. Figure 3.1B shows the number of connections assayed for each cell in this study, which conforms with previously published results (Butcher et al. 2012). Cells vary in the number of claws they possess but the vast majority have between 4-7 such claws, and in most cases the claws imaged are all the claws of a cell (we have not quantified the discrepancy between the number of claws imaged versus the number of claws the cell has, since it is not pertinent to our question).

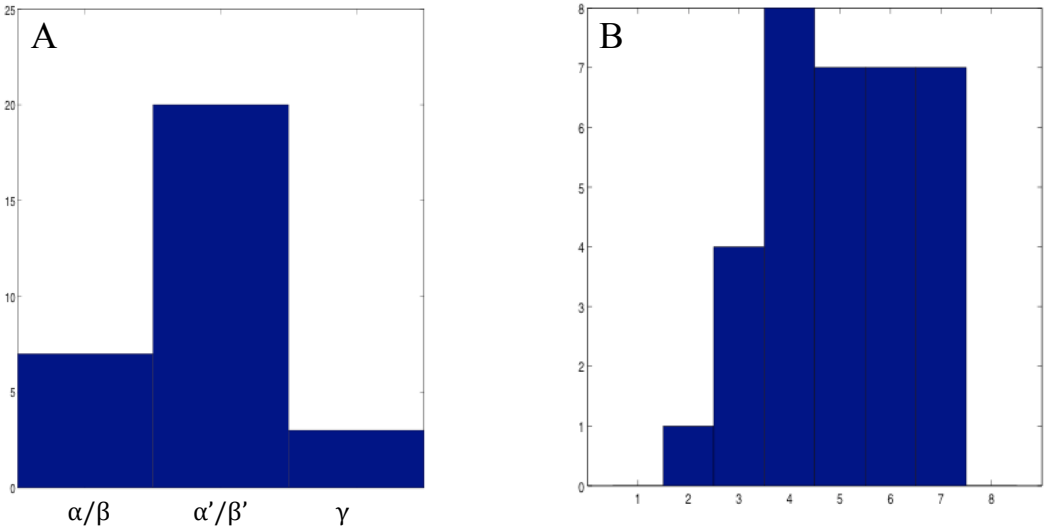

Figure 3.1 Properties of cells analyzed by functional imaging of dendritic claws and soma. **(A)** Distribution of the different cell types imaged. **(B)** Distribution of the number of claws imaged per cell

Next, we wanted to verify that we could detect odor responses in dendritic claws and that those responses would be reproducible. For that purpose we expressed GCaMP3 and myr-tdTomato in individual cells, identified their dendritic claws online, focused on each claw individually, and acquired their odor responses (Figure 3.2). The rationale for using the red channel was three-fold: (1) it allowed us to acquire a low-resolution z-stack and identify the location of the claws within that stack (2) while imaging responses, it allowed us to decrease laser power to the minimum so as to avoid bleaching and photo-damage (3) in the post-hoc analysis phase, the red channel provided an independent measure of image quality and consistency (see Methods).

Responses in the claws are easily identifiable and different odors evoke different responses (Figure 3.2A_{iii} vs. A_{iv} and B_{iii} vs. B_{iv}). Note that although the two claws depicted in Figure 3.2A are clearly from the same cell and are connected by a short neurite, they exhibit independent responses to the odors. Both claws show a strong response to apple cider vinegar, but only the right claw responds strongly to methylbenzoate (Figure 3.2A_{iii} vs. A_{iv}). Claws were not always imaged simultaneously, because of the difficulty of capturing them in the same plane, but when they were (as in this example), independent responses were evident (data not shown).

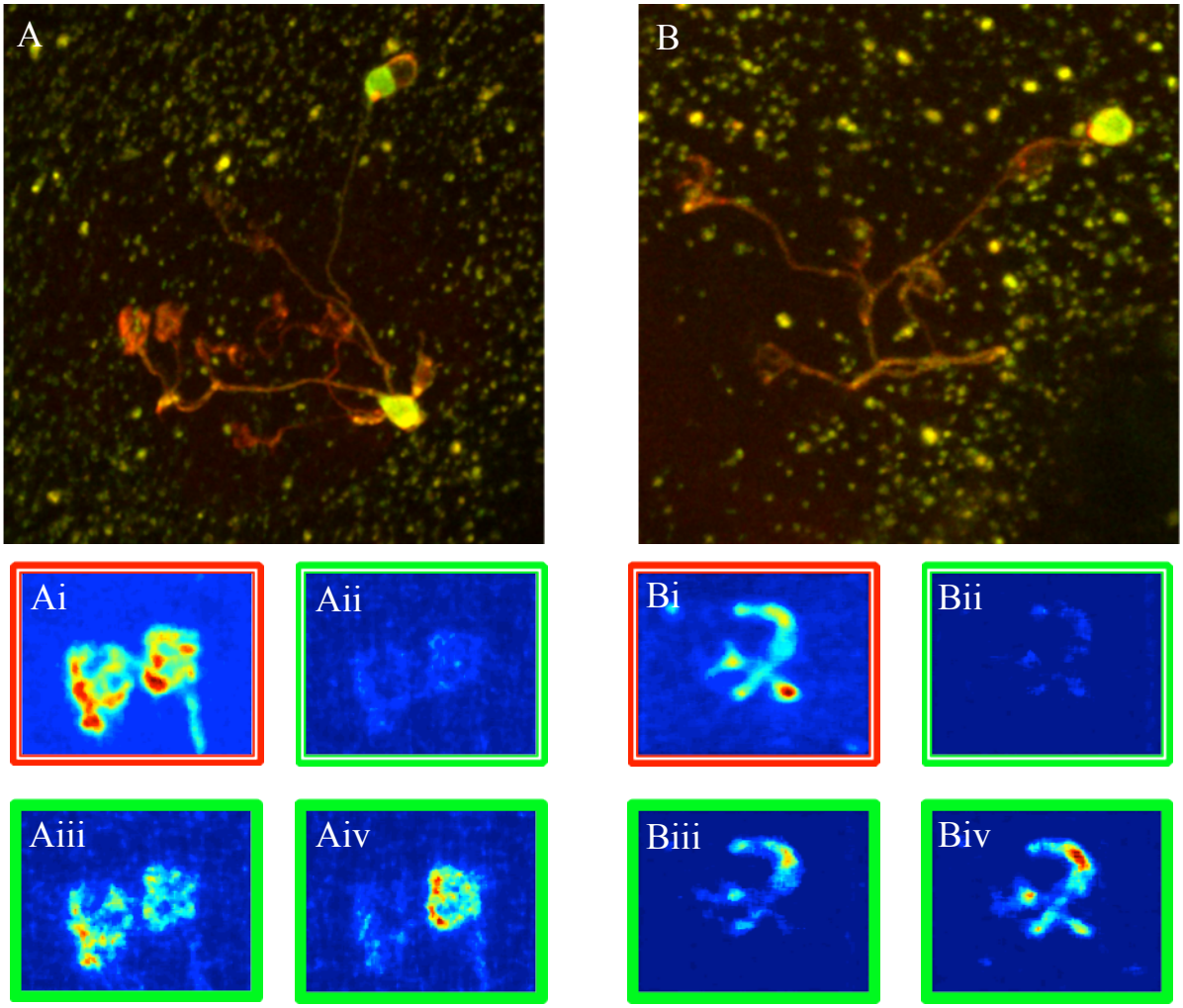

Figure 3.2 Independent responses to odors in dendritic claws. **(A,B)** maximum Z-stack projection of two example cells. Boxes demarcate the magnified region presented below. **(Ai)** Mean fluorescence image of 10 frames from the Red channel. **(Aii)** Mean fluorescence image of 10 frames for the green channel prior to odor exposure. **(Aiii)** Mean fluorescence image for 10 frames in response to apple cider vinegar. **(Aiv)** Same as Aiii only in response to methyl-benzoate. **(Bi-ii)** Same as Ai-ii but for corresponding cell. **(Biii)** Mean fluorescence image for 10 frames in response to orange. **(Biv)** Same as Biii only in response to pentyl acetate. For each cell the color scale is the same for all images.

Having identified responses, our subsequent goal was to quantify them and establish their level of reliability. We chose to calculate ΔG/R, since dividing by the red channel circumvented the problems arising from dividing by the much weaker green signal, which during the baseline period was close to zero (see again Figure 3.2A_{ii} and B_{ii}). Each claw was presented with 10 different odors and a clean air control 3 times in a pseudorandom manner (the same odor was never presented twice in a row). Odors were selected from different chemical classes and included 6 monomolecular odorants and 4 natural complex mixtures that were meant to increase the probability of seeing a response. Figure 3.3 shows the response curves to all the odors from a single claw. As can clearly be seen, the claw responded only to certain odors from the panel, and the responses are fairly consistent between repeats. We have quantified the responses by summing the area underneath the response curve that was above a baseline-derived threshold (for details see Methods). The figure shows the individual thresholds determined for each odor and each presentation, and also examples of false positive (third response to 2-phenylethanol) and false negative calls (third response to 1-hexanol). Having calculated the responses of all the individual claws to all the odors, we could now compare between the different claws from the same cell.

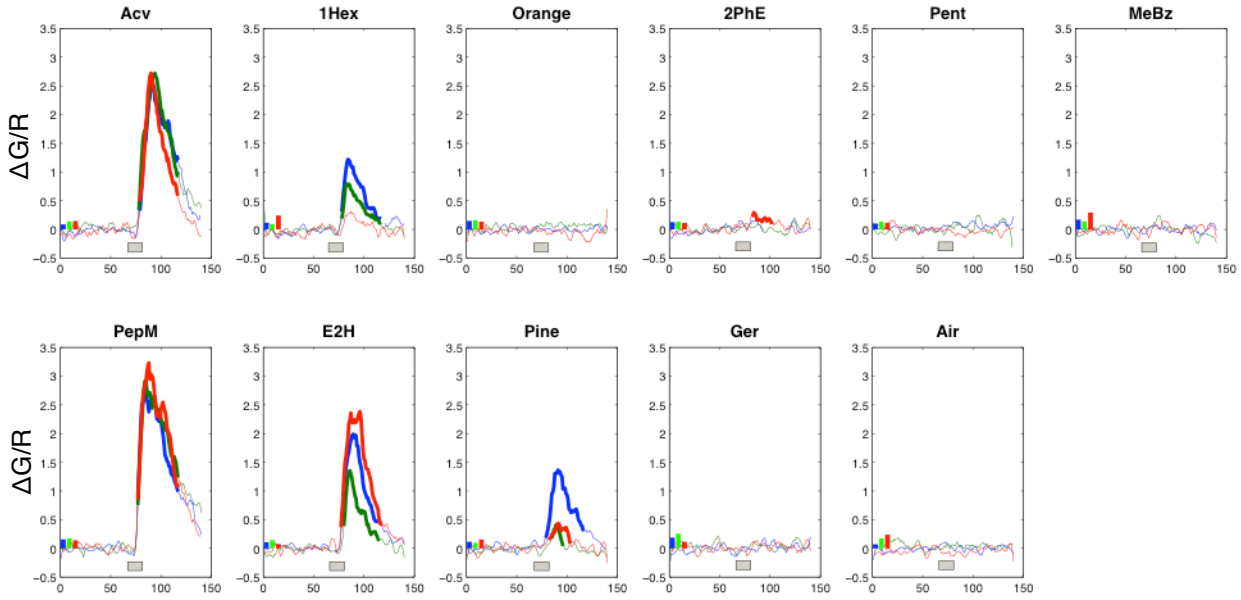

Figure 3.3 Odor responses from an individual dendritic claw. The plot presents all the data acquired from one claw. Each subplot is the response to one odorant, and each color represents a different odor presentation trial. X-axis is given in frames and Y-axis in ΔG/R. Odors were presented in a pseudorandom manner and grouped for display. Bold bars at the bottom left of each subplot represent the threshold for a significant response. Bold lines demarcate the frames that were used to calculate the response magnitude. Gray bars in each subplot delineate odor presentation.

3.4.2 Claws Exhibit Different Degrees of Similarity

If a single claw shows a well-defined tuning curve to our panel of odors, what are the responses of all the dendritic claws from a single cell? And, do all the cells show a similar level of correlation between their claws? To address these questions we first examine the entire response repertoire acquired from five example cells (Figure 3.4). Each row in the figure represents the data from a single cell, while each column is a claw from that cell (column are arranged based on the overall response magnitude). This plot also depicts the reproducibility of claw responses, since each dot denotes the magnitude for a particular trial and each bar is the median response. Qualitatively, it is clear that different cells display different degrees of similarity in their inputs. Cell 1, for example, seems to share just a single input channel, albeit a broadly tuned one. Cell 3 also seems to share mostly a single input channel, though this is a narrowly tuned channel that responds strongly just to apple cider vinegar. Cell 2 seems to receive a different input channel in each one of its claws (all relatively narrowly tuned). And cells 4 and 5 display a mixture of both phenotypes. Claws 7 and 5 in cell 5 have the same tuning curve, while claws 4 and 3 are highly dissimilar (note that claw numbers indicate the order in which they were imaged, while their position in the plot indicates magnitude of response).

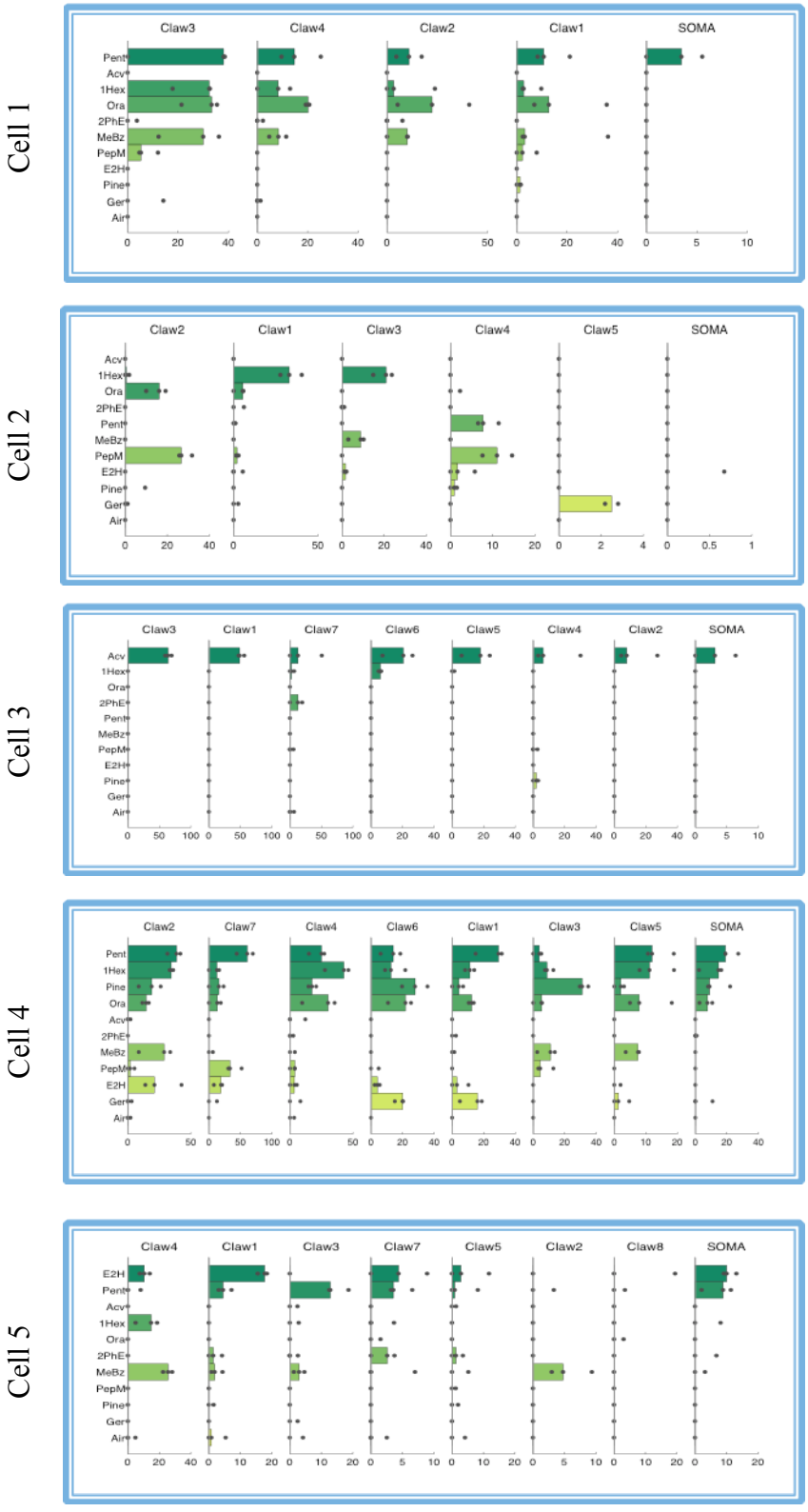

Figure 3.4 Dendritic claw tuning curves show evidence of both integration and amplification of input. The figure presents five example cells from the dataset. Each subplot is data from a single cell, while each column is data from a single dendritic claw. The X-axes are the magnitude of the fluorescence response (ΔG/R) and the Y-axes are the different odors. Claws are arranged from the strongest responding to the weakest responding, while odors are arranged by the somatic response for that cell.

To capture this qualitative impression of similarity between claw tuning curves we decided to use Kendall's τ as our rank-order correlation measure. Since this measure is not commonly used I will include a brief description of its logic and the reason we chose it. The algorithm for calculating the measure is as follows. First, one generates all the ordered pairs from the lists that are being correlated. For example, if the lists are {1,2,3} and {1,3,2}, then their ordered pairs will correspondingly be {[1,2], [1,3], [*2,3*]} and {[1,3], [1,2], [*3,2*]}. Next, one subtracts the number of all the discordant pairs from the number of concordant pairs (in our example: 2-1). Next, this number is normalized by all the possible non-ordered pairs for a list of that size (in our example: 3). Normalizing limits the measure to values between 1 (completely concordant) to -1 (completely discordant). A τ value is given by the formula:

$$\tau = \frac{\left(Number \quad of \quad Concordant \quad Pairs\right) - \left(Number \quad of \quad Discordant \quad Pairs\right)}{\frac{1}{2}N(N-1)}$$

The reason we chose this correlation measure was to be conservative in what we deem to be different tuning curves, as will become clear in the example in Figure 3.5.

The conversion from a set of tuning curves into a correlation matrix is displayed in Figure 3.5, with Figure 3.5A presenting the tuning curves of all the claws from a single cell, and Figure 3.5B presenting its corresponding Kendall's τ matrix in a color coded manner. The high degree of similarity between claws 1 and 2 is clearly captured by the measure. The similarity between claw 3 and claws 1 and 2 is still relatively high, which is because claw 3 could be regarded as a thresholded version of claw 1. Since thresholding can result from several technical differences (e.g different GCaMP levels in different claws, using a different laser power and/or a different PMT gain), we did

not want to regard it as stemming from a biological difference. Claw 4 however, both clearly represents a different input and has a very low correlation value.

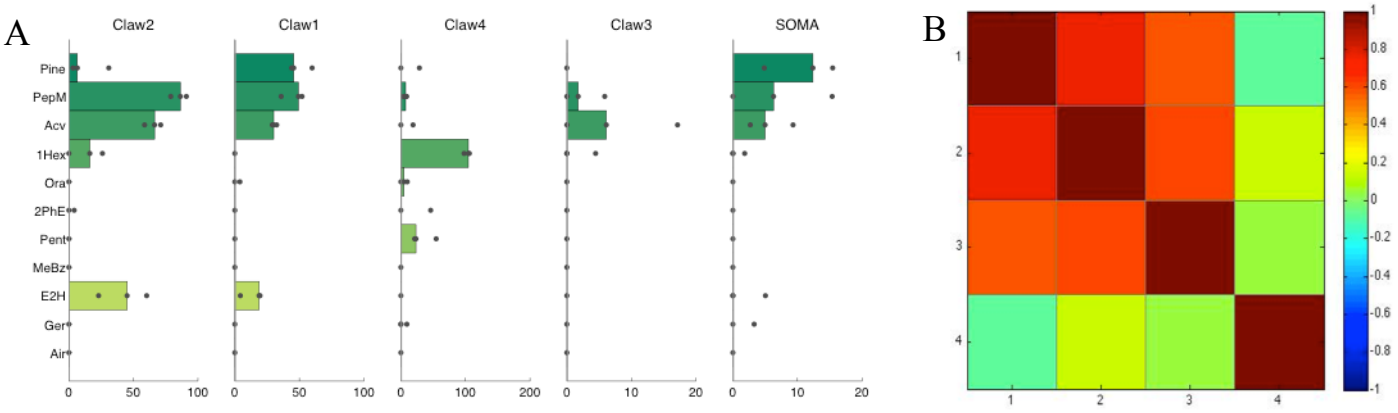

Figure 3.5 Determining odor tuning similarity across dendritic claws. **(A)** Example showing claw and somatic odor tuning of a single cell using the same conventions as in figure 3.4. **(B)** Correlation matrix (Kendall's τ) for the claw tuning curves from the cell in A. Notice that the soma is excluded from the analysis.

3.4.3 Kenyon Cells Receive Different Inputs

KCs with a high correlation values can be considered amplifiers, since most of the signal they receive is from the same PN channel. KCs with a low or negative correlation value are integrators, since most of their inputs are clearly different. Having measured the correlations between all the claws, we can now look at the overall distribution of correlation values within each cell. By considering the correlation distribution of each individual cell, we can see that there is no clear distinction between the 2 types (Figure 3.6A). The individual lines span a range from highly correlated to highly non-correlated, with no apparent discontinuity in between. Even within a cell we can sometimes see a combination of both extremes. The third cell from the top (Cell 32), for example, has identical inputs in all of its claws but one, which is highly uncorrelated (Figure 3.6A). Figure 3.6B shows a histogram of all the pooled pair-wise correlation values calculated for all the claws of each cell separately (the figure can be regarded as a projection onto the x-axis of the Figure 3.6A). Several observations are evident from this histogram. First, the correlation values span a wide range, from 1 (identical within the limits of our detection) to -0.5 (almost completely inverted rank order). Claws with a correlation of 1 display tuning curves like cell 1 in Figure 3.4. As can be seen from the histogram, there are several such cells. Claws with a correlation value of -0.5 show comparable similarity to that between the claws of cell 2 in Figure 3.4. Second, it is clear from the abundance of low correlation values that KCs do receive different input channels. Even if we consider only the stringent threshold of 0.2 as considerably different, we can see that more than 15% of the pairs get different inputs (though there is a statistical test for Kendall's τ, the limited number of odors tested and the even more limited number of actual responses in each claw decrease the power of the test considerably and make its use in this case irrelevant). Third, as is clear from the comparison between the experimental correlation values and the randomly generated correlations (Figure 3.6C) there are more high correlation values than expected by chance.

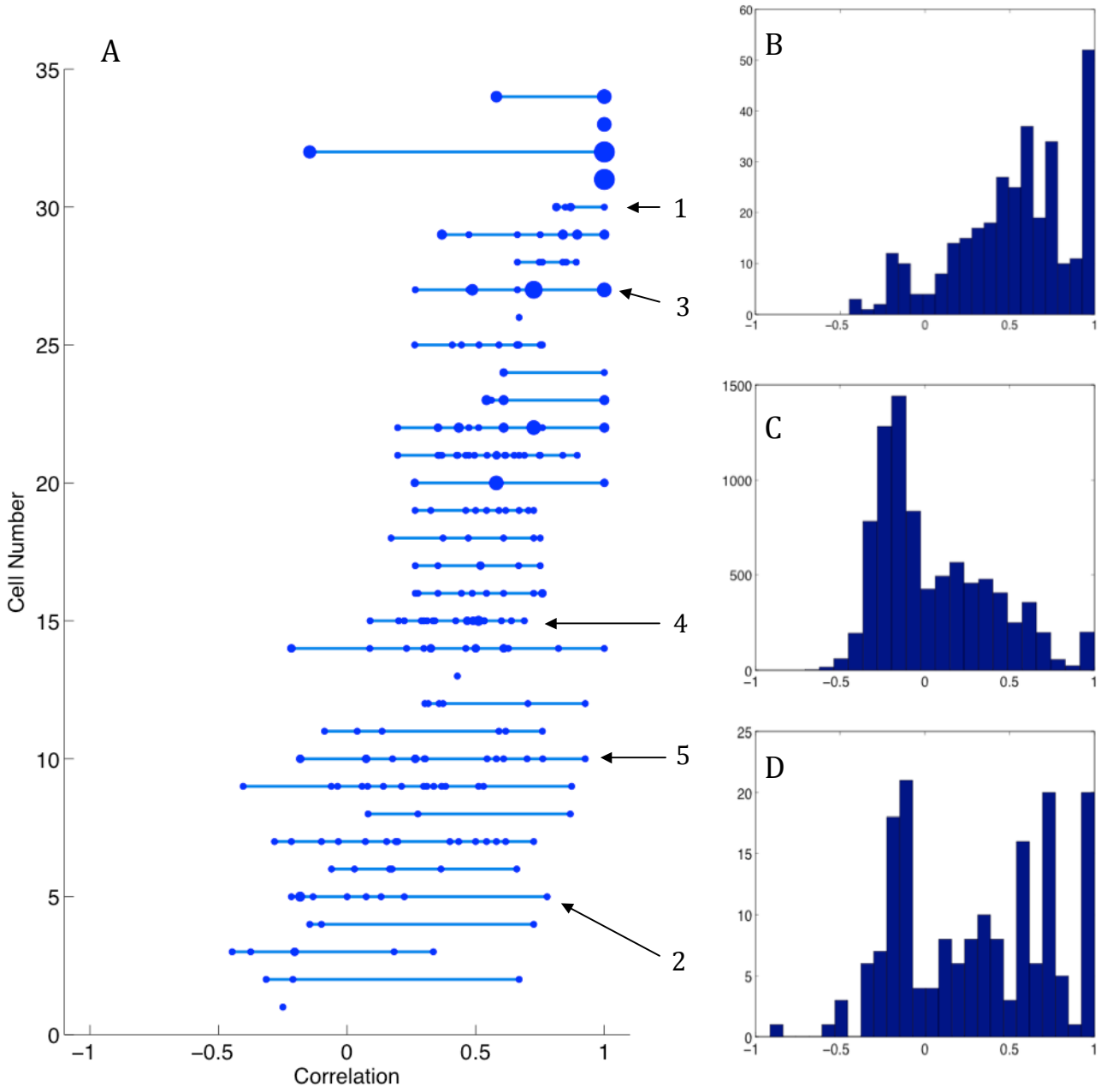

Figure 3.6 Odor tuning of different dendritic claws is distinct but more similar than chance. **(A)** Line depictions showing similarity of claw odor tuning (Kendall's τ) for all the cells. Each line is comprised of all the pair-wise correlations between the claws from a single cell. Dot on the line correspond to the correlation value of a single pairwise comparison from that cell, while the size of the dot indicates the number of pairwise comparisons that had the same value. Numbers at the right side of the plot correspond to example cells from figure 3.4. **(B)** Distribution of τ correlation values calculated for each cell separately and pooled. Effectively, a projection of the data in A onto the X-axis **(C)** Distribution of correlation values expected by chance. Distribution was generated by pooling all claws and randomly sampling from the dataset to generate virtual cells. **(D)** Distribution of correlation values observed in the dataset after excluding odors that evoke a somatic response (different odor(s) are excluded for each cell).

High correlation values could result from two different reasons: (1) KCs get different inputs but the inputs are more correlated than expected by chance. (2) Back-propagating action potentials that induce the same reaction in claws not because of similar inputs, but due to a shared output. To address the second possibility partially, we recalculated all the pair-wise correlations between the claws excluding all the odors that evoked a somatic response for that particular cell (Figure 3.6D). As can be seen, the distribution of τ values in Figure 3.6D still has higher correlation values than the random distribution, implying again stronger correlation than by chance alone. Though there are still certain caveats with this approach (GCaMP is not calibrated in these cells and so action potentials are not necessarily represented with a somatic response), these results indicate that the inputs are more correlated than by chance. In other words, KCs tend to sample PNs that have similar tuning curves, or possibly even sample PNs from the same channel more than once. We will postpone the discussion on the correlated inputs to the end of the next chapter, since it presents corroborating evidence.

3.5 Discussion

The olfactory modality has always been regarded as an intrinsically combinatorial sense. Inputs in the first layer of the system (both in flies and mammals) are broadly tuned and respond to numerous stimuli, while even simple monomolecular stimuli evoke responses in several ORN types. This implies that to generate the complete percept of an odor, integration between the channels has to occur. Based on our current knowledge of the fly olfactory system it was postulated that the majority of channel integration occurs in the KC layer. Using single cell 2-photon *in-vivo* imaging we were able to show that the inputs coming into different dendritic claws of the same cell are functionally distinct. Since the differences between the claws involved rank order inversions in their tuning curves, we deduce that KCs do, in fact, receive inputs from different PN channels. Interestingly, the level of correlations we saw between the claws from a single cell was higher than expected by

chance. Though we cannot prove this definitively, we believe the reason for that is due to inputs with correlated tuning connecting to the same KC. In other words, KCs receive different PN inputs but in a biased way – they tend to connect to PNs with similar odor tuning properties.

4 Kenyon Cells Functionally Integrate Inputs

4.1 Abstract

In the previous chapter we have shown that KCs receive inputs from different PN types, but do they really integrate those inputs in order to spike? If KCs function as obligate integrators in the olfactory pathway, only when all of their inputs are active will the KC spike. The experiment described below addresses the question of how many inputs are needed to drive a KC to spike. We used ChR2 to stimulate a small subset of PNs and recorded the evoked responses in single KCs using whole-cell recordings. By expressing YFP together with ChR2, and dye-filling the KC during the recording, we were able to correlate the response evoked with the number of physical connections between the PN subset and a particular KC. Our results show that responses become stronger and more reliable when three or more connections are active. By examining responses to individual spikes we also show that integration between claws is more efficient than integration within a claw. Finally, by looking at the distribution of the number of connections, we are able to corroborate our finding from the previous chapter that KCs' connection to PNs is biased.

4.2 Background

KCs are notorious for their sparse responses. When compared to the earlier layers in the pathway (ORNs and PNs), KCs respond to fewer stimuli, with fewer spikes, and with fewer cells in the population responding to any particular odor (Murthy et al. 2008; Turner et al. 2008; Honegger et al. 2011). Though this response pattern is characteristic of higher brain regions, it is still unclear how

KCs achieve this level of sparseness. In the previous chapter we have shown that KC claws have different odor tuning curves, and therefore that an individual KC receives input from more than one PN type. However, we do not know if KCs actually require those different inputs in order to spike.

Considering the particular anatomy of a KC it seems unlikely that the activation of a claw will have no impact on the spiking properties of a cell. This seems especially true if we recall that each KC claw forms more than 20 active zone contacts with a single PN bouton (Leiss et al. 2009). Since dendritic claws are the main source of input for a KC, and since each KC only has between 5-7 claws that are comparable in size to its soma, evidence for different inputs in the claws strongly support functional integration in KCs. However, it is still unclear how many of the inputs need to be active to induce KC spiking and how strongly they need to fire to drive the KC above spike threshold.

For the purpose of this experiment, we chose to drive ChR2 in a subset of PNs using the Mz19 driver line. We chose this line since it drives expression in 3 out of the 54 different PN types (Jefferis et al. 2004). The labeled glomeruli themselves (VA1d, DA1, DC3) are of less consequence for our purpose. Rather, this line provides us with strong and sparse expression in the PN layer. Strong expression ensures that we will be able to drive PN activity to levels comparable to an odor stimulus; and sparse labeling ensures that we are able to detect individual connections between PN boutons and KC claws. Naturally, there are sparser lines, but those will reduce the probability of finding a connection.

Although we are using light microscopy to detect synaptic connections, we believe that considering the unique KC anatomy, it is tenable. Each individual dendritic claw is usually a large complex structure that forms multiple connections with a PN bouton (~5μm in diameter). Therefore, identifying a single connection will usually entail an overlap between 2 complex structures across several frames of a confocal stack (see Figure 4.5). While not providing the same degree of certainty as electron microscopy reconstruction, we believe that it is sufficient for our purposes.

4.3 Methods

Fly strains

Flies used in this experiment were 5-7 day old heterozygous females generated from the Gal4-Mz19 (Tanaka et al. 2004) to UAS-ChR2-YFP (Hwang et al. 2007) cross. Flies were collected on the day of eclosion and transferred onto agar plates where they were supplied with yeast paste supplemented with 5mM all trans-retinal. The flies were then reared in the dark for 2 days, supplemented with a fresh plate of yeast paste retinal, and used for recordings for the next 2 days.

Animal preparation

For KC whole cell recordings flies were positioned in the same angle as described in section 3.3. The antennae were surgically removed to reduce baseline activity and facilitate identification of photostimulation-evoked activity (Olsen et al. 2007). For PN cell-attached recordings, flies' head was tilted backwards so that the antennae appeared on the upper side of the recording platform. The cuticle cover between the eyes and the antennae was removed completely to expose the antennal lobes. Extracellular saline used for both preparations was identical to that described in the previous chapter.

Whole cell and cell attached recordings

The saline in the recording electrode contained (in mM) 125 L-K aspartate, 10 HEPES, 1.1 EGTA, 0.1 CaCl2, 4 MgATP, 0.5 Na3GTP, and for the whole cell recordings 250μM Alexa568 hydrazide was added fresh to the internal solution prior to each experiment (internal solution osmolarity was adjusted accordingly). Details for KC recordings are described elsewhere (Turner et al. 2008). Cell-attached PN recordings were done under similar conditions with marginally bigger pipettes to impede spontaneous break-in. A strong current pulse (500pA for 500ms) was delivered at the end of the recording to verify that no spikes are generated and no spontaneous break-in occured. Selection criteria for KC whole cell recording included both the quality of the recording and the

possibility of a connection. For quality control we have injected each cell with a current ramp and determined the spiking threshold at three separate times throughout the experiment. Cells in which spikes could not be detected were excluded from the analysis. Though some cells with no connections were analyzed fully in this experiment, we often aborted the recordings of cells that did not show any sign of functional connection. If after three repeats of the entire stimulus set, there was not obvious response in the KC, the recording was aborted and the cell was not processed any further.

Tetrodotoxin (TTX) and Mecamyamine were applied to the bath by mixing them into the regular bath saline at a concentration of 1μM and 100μM, respectively. Solutions were prepared fresh from a frozen concentrated stock prior to each experiment.

Light stimulation

Light stimulus was delivered using a THORLABS high-power LED driver (LEDD1B) driving a blue LED (470nm) at 1Amp, mounted on a THORLABS collimated LED holder (LEDC1). We used a Matlab code to control stimulus duration. Light was delivered through the objective and bathed the whole preparation.

Confocal imaging

After data acquisition, the brain was dissected out of the head capsule and immediately transferred to a Phosphate Buffer filled vial. Para-formaldehyde was then added to the vial to a final concentration of 4% and the brain was rocked for 10min at room temperature. After fixation, the brain was washed three times with phosphate buffer and mounted directly on a slide using Vectashield (VECTOR laboratories). This particular protocol was chosen as a compromise to get reasonable anatomical information from both PNs and KCs. The Alexa signal (labeling the KC claws) was reduced dramatically if triton was added to the washing steps. The YFP signal could not be augmented with immunocytochemistry, since without triton antibodies did not penetrate the tissue properly. Several attempts were made to image the brain directly without any fixation, but although the Alexa signal was of high quality, severe damage to the boutons will sometimes ensue under these conditions. Confocal images were acquired using a ZEISS LSM-510 microscope with a 63X oil

immersion objective. Identifying connections between PN boutons and KC claws was done manually in a blind manner using the ImageJ software (Abramoff et al. 2004).

Data analysis

All data analysis was performed in Matlab (MathWorks 2010). Spikes were identified using a filtering and time-derivative based algorithm. Due to the relative small size of KC spikes, all traces were also corrected manually for both false positive and false negative calls of spikes. To calculate response magnitude, the mean trace for a particular stimulation duration was calculated and the baseline value was subtracted from the maximal value during the stimulation period. Spiking response was calculated in a similar manner. The number of spikes for a particular stimulation regime was calculated as the mean number of spikes during a window that included the stimulation period plus 200ms (since spikes were seen to occur sometimes right after stimulation offset) minus an equivalent time frame prior to the stimulation.

4.4 Results

4.4.1 Calibrating PN Responses to Light Stimulation

For this experiment to be informative, we needed to verify that we would be able to drive PN spiking in a way that is comparable to odor stimulation. Based on pervious published results (Wilson et al. 2004; Bhandawat et al. 2007), PN responses can reach 200Hz directly after odor onset. We have explored different stimulation regimes so as to try and maximize the yield of spikes from a constant light intensity. Other studies have shown that intrinsic adaptation of ChR2 can decrease its conductance by more than half, and that interleaving the stimulation with dark periods might alleviate the problem (Grossman et al. 2011). We, therefore, recorded from ChR2-YFP expressing PNs, visually guiding the pipette to the YFP-labeled cells that were either dorsal or lateral to the antennal

lobe, and tried different stimulation regimes. The underlying principle was to try using the shortest stimulation that induces a reliable response, while interleaving it with the shortest dark periods that would allow for the recovery of the response.

Figure 4.1A shows the response of one PN to constant stimulation with different light durations. Though the response is clearly reliable, it does show a detectable adaptation after more than 25ms and a loss of entrainment as stimulation duration increases. Although we have tested several different stimulations regimes (Figure 4.1B), we were unable to induce a faster spiking response (after the dark periods have been accounted for). Fortunately, even with a constant light stimulation, the spiking rate evoked in the PNs was similar to that evoked by a strong odor response (Figure 4.1C).

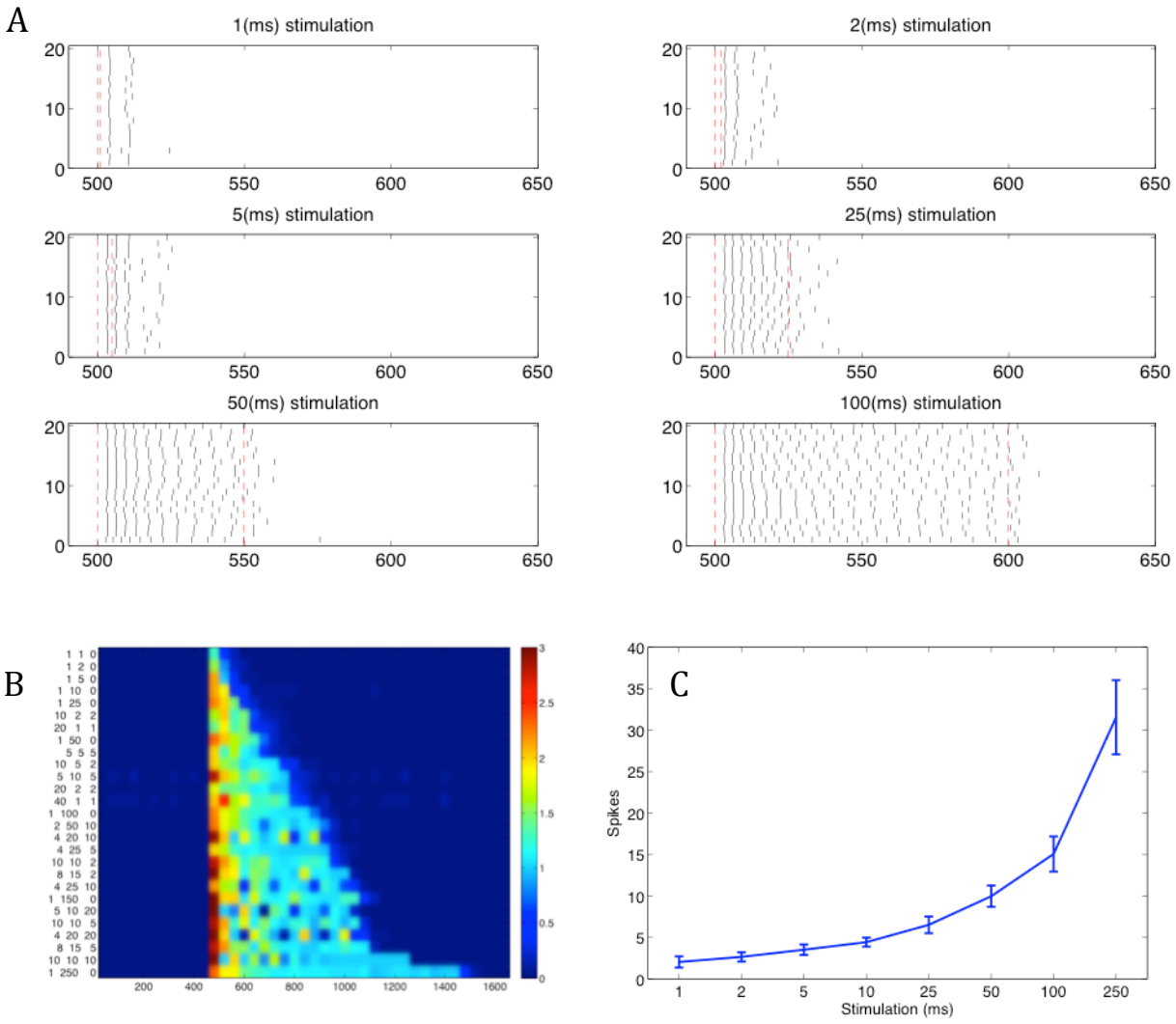

Figure 4.1 Light stimulation induces reliable responses in PNs. **(A)** Raster plots from a single PN showing responses to six different stimulation durations. X-axes are time in ms, and Y-axes are trial number. Red lines demarcate light stimulation. As can be seen, evoked responses are highly reliable. **(B)** Mean PSTH for different stimulation regime. Each row is the mean of one stimulation regime applied on different cells (N=8). The 3 numbers next to each regime represent: 1st – number of times regime was repeated; 2nd – light on period; 3rd – light off period. Colors represent number of spikes in a bin. Note that recovery of fast spiking is always preceded by prolonged silence. **(C)** Light evoked spiking responses in PNs for stimulation duration chosen for the study (N=8).

4.4.2 Characterizing KC Responses to Light Stimulation

Having established a stimulation regime in the PN subset, we turned to record the evoked responses in the postsynaptic KCs. In the previous experiment we could not control the number of claws stimulated and the strength of their stimulation. Therefore, any somatic responses that were seen could have been the result of several independent variables. Since the stimuli were different odorants, changing an odor could change both the number of claws stimulated and the magnitude of their response. With the experiment detailed below, we achieved a finer level of control over the stimuli. Although we cannot excite individual connections separately on the same KC, we can control the stimulation strength a cell receives and can compare cells with different number of connections.

The traces displayed in Figure 4.2A are an example of the graded response evoked by the light stimulation. In this particular example even the shortest stimulation evoked a detectable response. The figure shows how the input is gradually being summated until, eventually, the strongest stimulation evokes a spike. Note, that due to the unipolar nature of insect neurons, and the relative small size of the KC somata, the spike is detectable but small in amplitude. The traces displayed in Figure 4.2B exemplify additional characteristics of the data. First, even in individual traces it was sometimes possible to perceive the inputs being summated. Each step is indicative of an additional EPSP and its magnitude. Second, the two repeats from the cell indicated in red show that even a stimulation that was strong enough to evoke a spiking response did not necessarily evoke a consistent response. Finally, and most importantly, both panels of the figure show that ChR2 stimulation in a PN subset can be sufficient to drive a KC to spike.

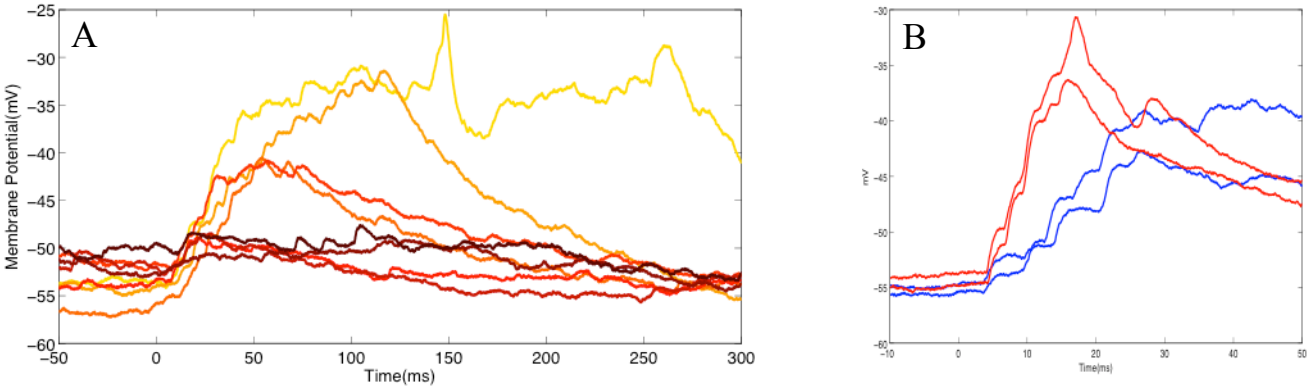

Figure 4.2 Evoked responses in Kenyon cells. **(A)** Membrane potential responses of one KC to a series of increasing photostimulation (1, 2, 5, 10, 25, 50, 100, 250 ms duration). Colors become brighter as stimulation duration increases. Note that the strongest stimulation induces a spike. **(B)** Examples of post-synaptic responses evoked in two different KCs (red and blue). EPSPs are clearly visible in each recording. Note different time scale from A.

To assess the overall effect the stimulation induced in different KCs, we chose to calculate two separate parameters for each light duration – mean magnitude of response and mean number of spikes evoked (see Methods). Figure 4.3A displays the summary of all the trials recorded from the cell in Figure 4.2A. The mean response is depicted by the red line and the magnitude was calculated as the difference between the peak and the baseline. The number of spikes evoked is shown in a raster underneath each response plot, with the mean being calculated with respect to the baseline (the characteristic baseline firing rate was zero). As with the individual traces (Figure 4.2A), it is clear also from the mean that the response gradually builds up and that the spiking response evoked in this cell is not highly consistent. Different cells, however, showed different response patterns.

Considering just the spiking response, we can describe the pattern displayed by the example cell in Figure 4.3A as non-consistent. Figures 4.3B and 4.3C show examples of two different spiking responses: consistent and biased. In the consistent case, the cells responded with spikes to more than 80% of the trials (Figure 4.3B). Cells with a biased pattern, had a low baseline-firing rate; spiking was entrained to the light stimulation epoch but overall spike rate did not increase much (Figure 4.3C). Focusing on the mean response of each cell, we can see a clear hyperpolarization in both Figure 4.3A and 4.3C. This pattern was characteristic for our dataset, although some cells did not display it (e.g. Figure 4.3B) and some showed just a strong slow hyperpolarization with no excitatory response. Overall, our dataset contains 39 cells that were connected but could not be driven to spike, 5 that showed biased spiking, 10 that showed non-consistent spiking (sometimes with just a few spikes), and 6 that showed consistent spiking. Unfortunately, we were not able to recover anatomical information from all the recorded cells, and due to Murphy's Law, most of the cells that lack an image are consistently spiking cells.

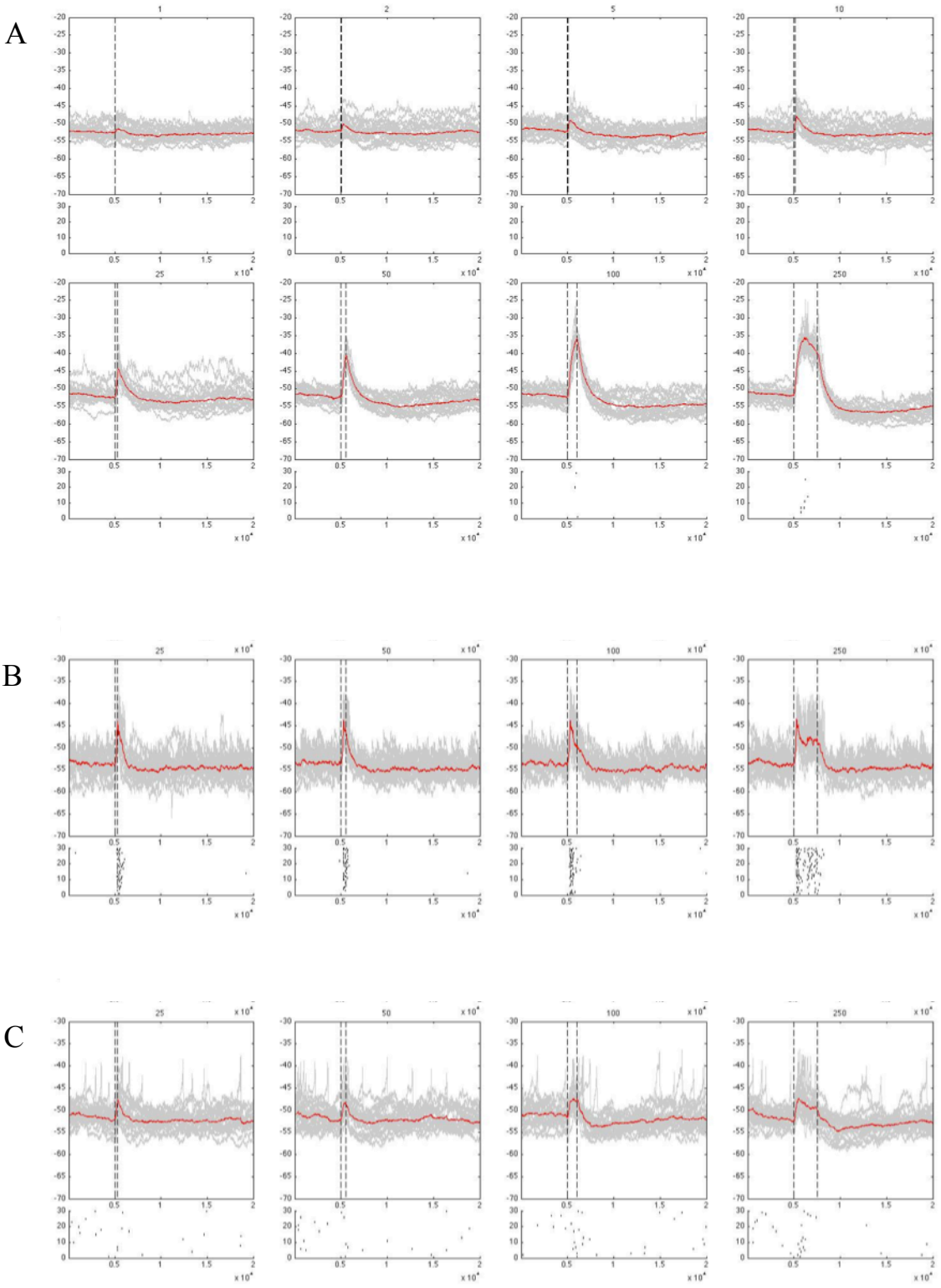

Figure 4.3 Types of spiking responses in Kenyon cells. **(A)** Response summary from a single cell that spiked sporadically. Each subplot shows KC membrane potential from individual trials in gray and the mean response in red. Title for each plot lists the stimulation duration. Bottom panels display raster plots of KC spiking. **(B)** Same as in A only for a cell with a reliable spiking response. Note only four longest stimulation durations are presented. **(C)** Same as in B only for a cell with biased spiking response.

As mentioned, most of the cells showed a wave of hyperpolarization following the stimulation. Some cells displayed hyperpolarization with no apparent excitation and without having any connections to the excited PNs. This hyperpolarization is probably a result of a global inhibitory signal related to the general level of activity in the calyx (possibly the GABAergic APL neuron, (Liu and Davis 2008). It is worth noting that not all hyperpolarization seemed to originate from a global signal. As part of the quality control process in this experiment, every cell was injected with an increasing current ramp to induce spiking. Though this stimulated only a single cell, if the ramp induced more than a few spikes, a strong hyperpolarization followed, which could last several seconds (data not shown).

The responses displayed so far are a result of light stimulation applied to the entire brain of the fly. To verify that the responses recorded at the KC somata were a result of PN spiking, we applied both TTX and mecamylamine to the bath after the data acquisition phase. Application of mecamyamine alone (at 100μM) abolished most of the responses and left only a small transient that was probably a result of either the photoelectric effect or ChR2 evoked Ca^{+2} release (Figure 4.4A). This verified that the response is a result of activation of nicotinic acetylcholine receptors on the KCs, as should be the case if PNs are driving the response (Yusuyama et al. 2002). When TTX was applied to the bath (at 1μM), the response was also completely abolished (Figure 4.4B). This result verifies that it is the spiking activity of the PNs that drives the response, and not simply the activation of PN terminals. There have been several cases in which application of TTX did not block the response completely (Figure 4.4C). In these cases, responses were usually seen only in the two longest durations of stimulation (100ms and 250ms) and their profile was different than the ordinary response profile. Instead of a sharp rise and a steady state throughout the stimulation period, a gradual and steady increase throughout the duration of the stimulation. Interestingly, these responses were usually associated with cells that had multiple connections (mostly three and up) and they were abolished completely by the additional application of mecamylamine to the bath (Figure 4.4D). Taken together,

these data suggest that though it is possible to drive KCs by artificially releasing from the PN terminals, the responses evoked in this study are mainly the result of evoked spiking in the PN subset.

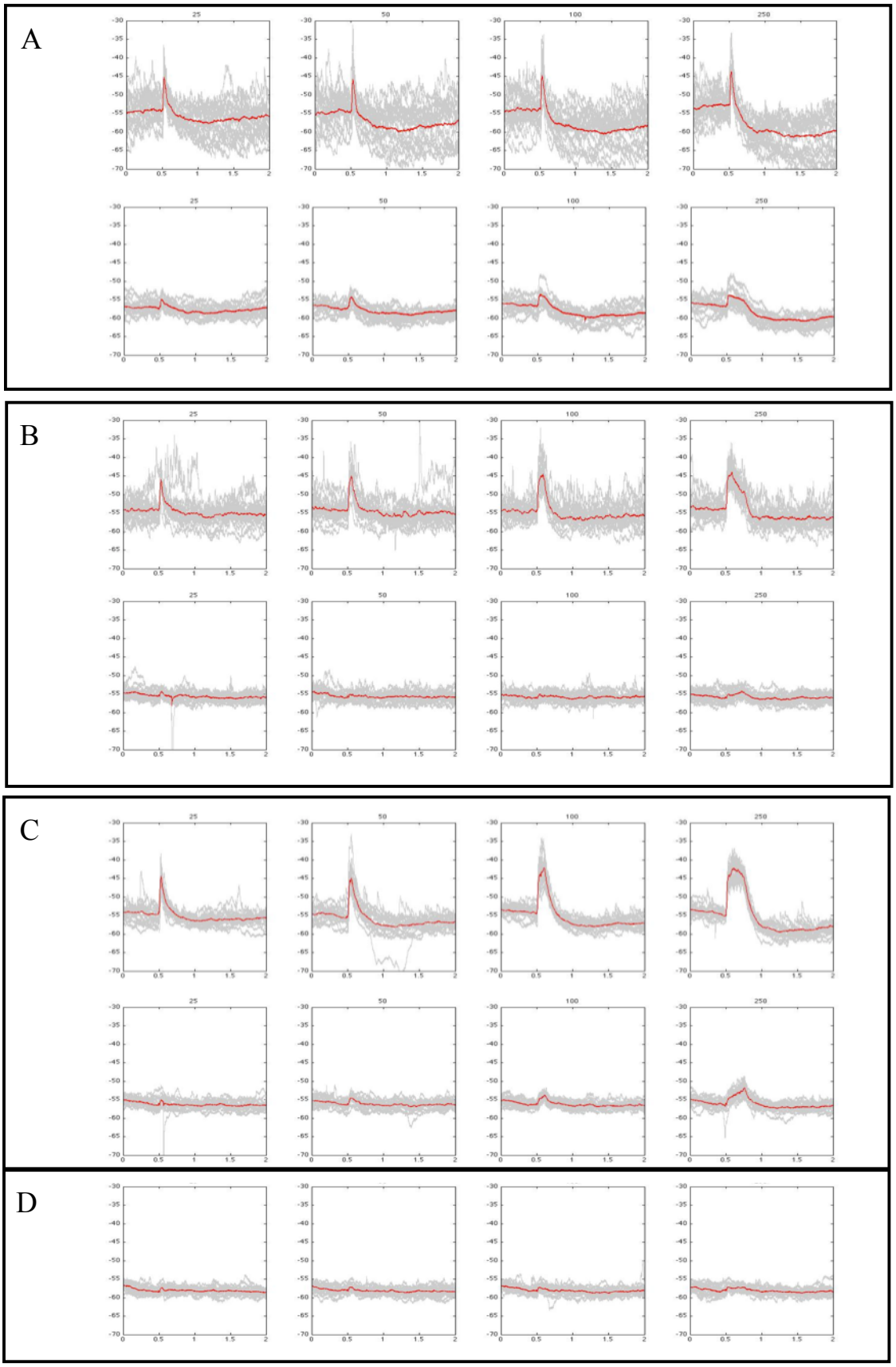

Figure 4.4 Light evoked responses are mediated by spike-dependent cholinergic transmission. Traces present KC membrane potential in response to the four longest stimulation durations. **(A)** Evoked response before (top) and after (bottom) bath application of 100μM mecamylamine. **(B)** Evoked response from a different cell before (top) and after (bottom) application of 1μM TTX. **(C)** Same as B only a small residual response can be seen after 1μM TTX application. **(D)** Same cell as in C supplemented with 100μM mecamylamine.

4.4.3 Claws and Boutons Show Complex Connections

Having characterized the functional part of the experiment we now turn to characterizing the anatomical part. As mentioned in the Methods section, ChR2 expressing PNs were labeled with YFP, while the postsynaptic KC was labeled with Alexa. Images were scored without knowledge of their functional responses to avoid any bias when determining the number of connections. While identifying claw-bouton connections, we have noticed that they are comprised of several distinct types. Even though we chose to regard only the number of connections and not their type, it is certainly possible that other aspects of the claw-bouton interaction are important in governing the strength of the connection. Figure 4.5 displays the three types of connections we have identified in this study. The first, and most common type is of an interleaved connection (Figure 4.5A). The claw wraps around the bouton sending fine processes that seem to sometimes merge with the bouton itself. The second most common type can be described as a cup-shaped claw (Figure 4.5B). In this type the claw forms a cup-shaped structure that nestles the bouton in its bosom. In the third type, which was the least common of all, the claw wraps specifically around the base of the bouton (Figure 4.5C).

Apart from identifying different connection types, we have observed a surprising finding – a single claw is not always a single input. A recent study has categorized claws into simple and complex forms based solely on their structure, and still assuming that a claw is a single unit of input (Butcher 2012). We have encountered several examples of complex claws, and in a few of these (< 10) we noticed contact to more then one bouton. The examples presented in Figures 4.5D and 4.5E show claws that contact two boutons from the labeled subset. The example in Figure 4.5F represents an even more striking result. This claw does not only contact more than one bouton, but the second bouton it contacts is not labeled by the Mz19 line. In other words, this claw is a clear example of integration occurring already within a single claw. This finding has prompted us to revisit our imaging data looking for sub-regions within complex claws that respond differently. Unfortunately, our temporal resolution does not allow differentiation on that scale. It is important to note, however,

that this finding does not detract from our conclusions –quite the contrary. It only makes a stronger case for integration of different PN inputs within a single KC.

Another aspect of the claw-bouton connection that showed large variability was the size of the connection itself. This will not be presented in a figure, since it was not quantified, but suffice to say that several claws were either exceptionally big or exceptionally small (when compared to other claws from the same cell). Although the size of the claw usually was an indication of a complex structure that might form connections with more then one bouton, we observed several instances where a large claw contacted a correspondingly large single bouton.

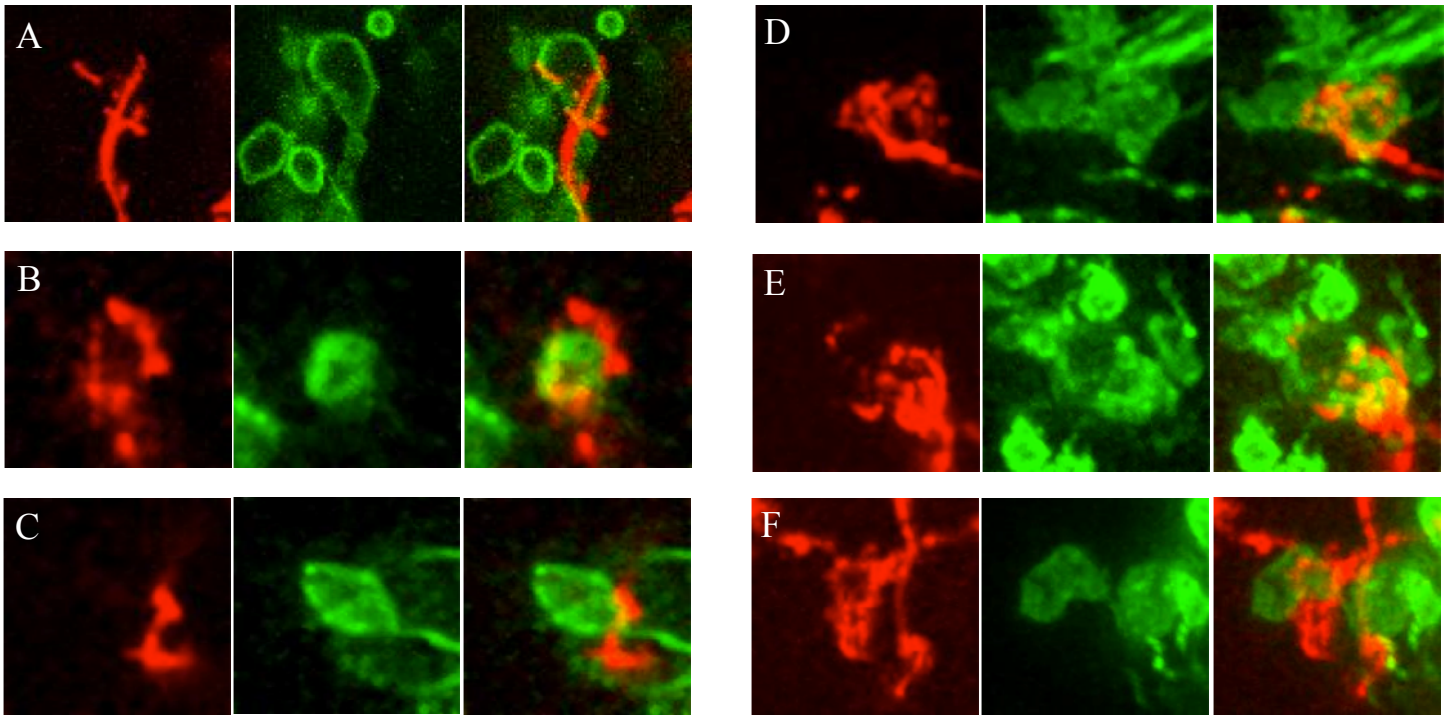

Figure 4.5 Dendritic claws show different modes of contact with PN boutons. **(A)** Dendritic claw interleaved around a PN bouton. **(B)** Cup-shaped claw. **(C)** Claw enfolds around base of bouton. **(D)** Complex claw with major (right) and minor (left) structures, each contacting a different bouton. **(E)** Same as in D only with minor structure on the right side. **(F)** Claw wrapping around base of bouton, while having room for another contact. Note that contact is from a different PN type. For panels D-F several frames were required to generate the Z projections, and therefore the boutons appear more blurry.

4.4.4 Kenyon Cells Require Three Active Connections to Fire Reliably

So far we have gleaned insight from the functional and the anatomical datasets separately. We shall now consider the two datasets concurrently with the hope of gaining additional understanding into the workings of the mushroom body calyx. Cells that do have both functional and anatomical data allow us to relate them and address the question we have set out to answer – how many claws need to be active for a KC to fire? Figure 4.6 displays exactly that.

The threshold for activating a cell is not a clean and sharp boundary (Figure 4.6A). Though it is possible to evoke spikes with just one connection being driven, the reliability of spiking increases with the number of connections, while the strength of the stimulation needed to induce a spike decreases. Note, however, that it is only for cells with three or more connections that we see the 75th percentile (top part of boxplot) clearly above zero. In other words, it is only with three or more connections that the spikes are produced in a reliable manner.

If we now turn to consider not only the spiking response but also the magnitude of the evoked response, we can partially explain the reason for the soft spiking threshold. Examining the responses evoked by all the cells based on their number of connections, we can see that the response tend to get bigger with the increase in the number of connections (Figures 4.6B-E). However, there are also several notable cases where a cell with few connections responds more strongly than a cell with more connections. A prominent example can be seen in Figure 4.6B, where a cell with a single connection surpasses all other recorded responses (compare to Figures 4.6C-E). This can be attributed, in part, to the different anatomical types of claw-bouton connections we have observed. It is entirely possible that bigger claws form stronger synapses, that interleaved claws are easier to excite, or that complex claws actually require both inputs to be active.

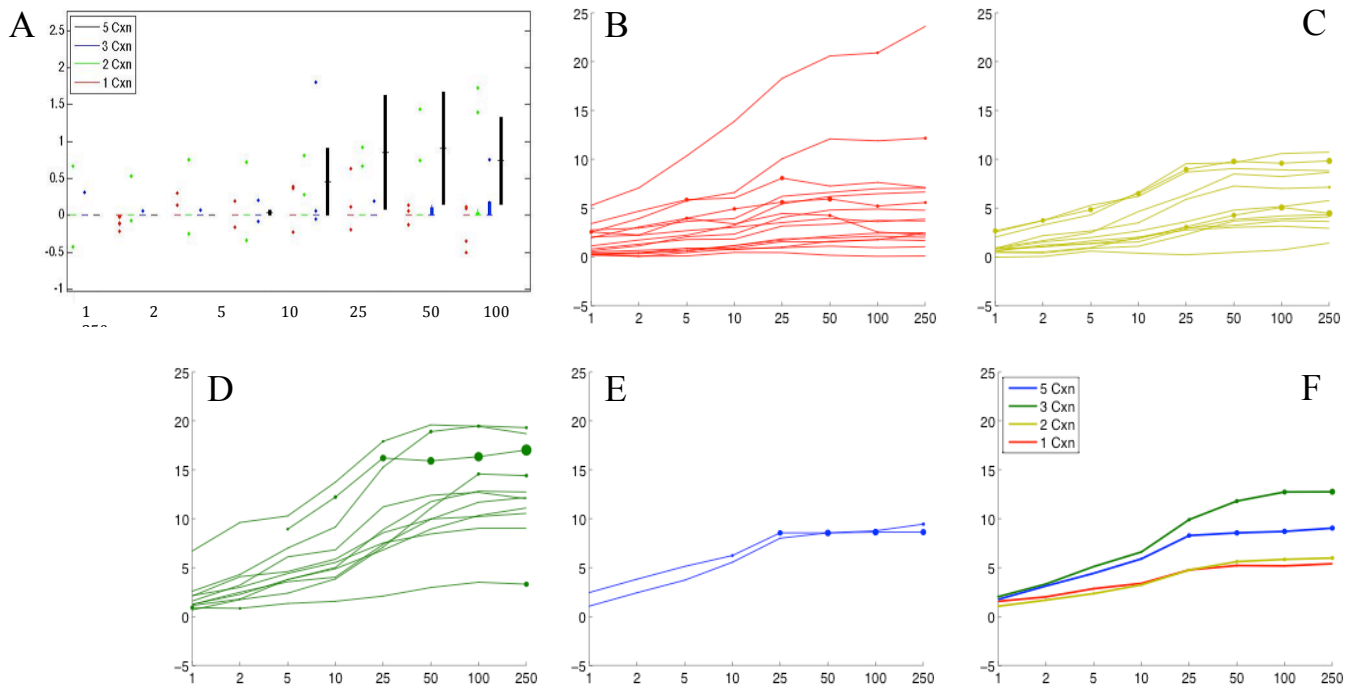

Figure 4.6 Spiking probability and response magnitude increases with the number of connections. **(A)** Boxplot representation of mean number of spikes evoked per stimulation duration and per number of connections. Dots represent outliers. Note that in most cases, KCs did not spike, so most boxplots are simply lines centered at 0. We found 16 KCs with a single synaptic contact, 12 with two contacts, 11 with three, and 2 with five. **(B)** Mean evoked response for all the cells with 1 connection. Each line represents the response amplitude (mV) of one cell across a range of different stimulus durations (ms). Dots on the line indicate a spiking response, with the size of the dot proportional to the evoked number of spikes. **(C-E)** Same as in B, only for KCs showing 2, 3 and 5 synaptic connections respectively. **(F)** Mean evoked response and mean evoked spiking for all the cells, with different connection numbers indicated by line color.

Another likely source for the fuzziness in the number-of-inputs boundary is the variability we encountered in the spiking threshold itself. Most KCs rest relatively far from spiking threshold, and therefore even evoked responses that were 20mV in size did not induce any spiking. However, some of the recorded KCs were either very close to spike threshold or even had a low baseline firing rate. Naturally, since there was no correlation between intrinsic spiking threshold and the number of connections with our PN subset, this added to the observed variability. Nevertheless, by examining either the distributions of evoked responses per connection (Figure 4.6B-E) or the mean evoked response (Figure 4.6F), we see that three or more connections induce considerably stronger responses. Having one or two connections is practically indistinguishable in terms of the response magnitude. But, as with the evoked spiking responses, adding the third connection seems to change the response distribution in a supra-linear manner.

4.4.5 Kenyon Cells Integrate More Efficiently Across Dendritic Claws

We now direct our attention to the lower end of the stimulation spectrum to probe deeper into the mechanics of integration in the mushroom bodies. PN responses to these short stimulation durations provide an opportunity to address the efficiency of temporal versus spatial summation in KCs. When stimulated with just 1ms of light, PNs produce a single reliable spike with a latency of about 4ms (Figure 4.7A). The second spike is produced with a lower reliability (~20% failure rate) and with a longer latency (a median of more than 10ms). There is typically no third spike, but if present it arrives with latency greater than 20ms. Increasing the stimulation to 2ms increases the reliability of the second spike to 100% and reduces its latency. Increasing it to 5ms generates three reliable spikes with a latency of less than 15ms for the third spike (Figure 4.7A). The results are even more striking if we consider the evoked responses in individual PNs (Figure 4.7B). Focusing on the response differences between these short stimulation durations allows us to ask what is a more efficient type of integration in KCs, temporal or spatial?

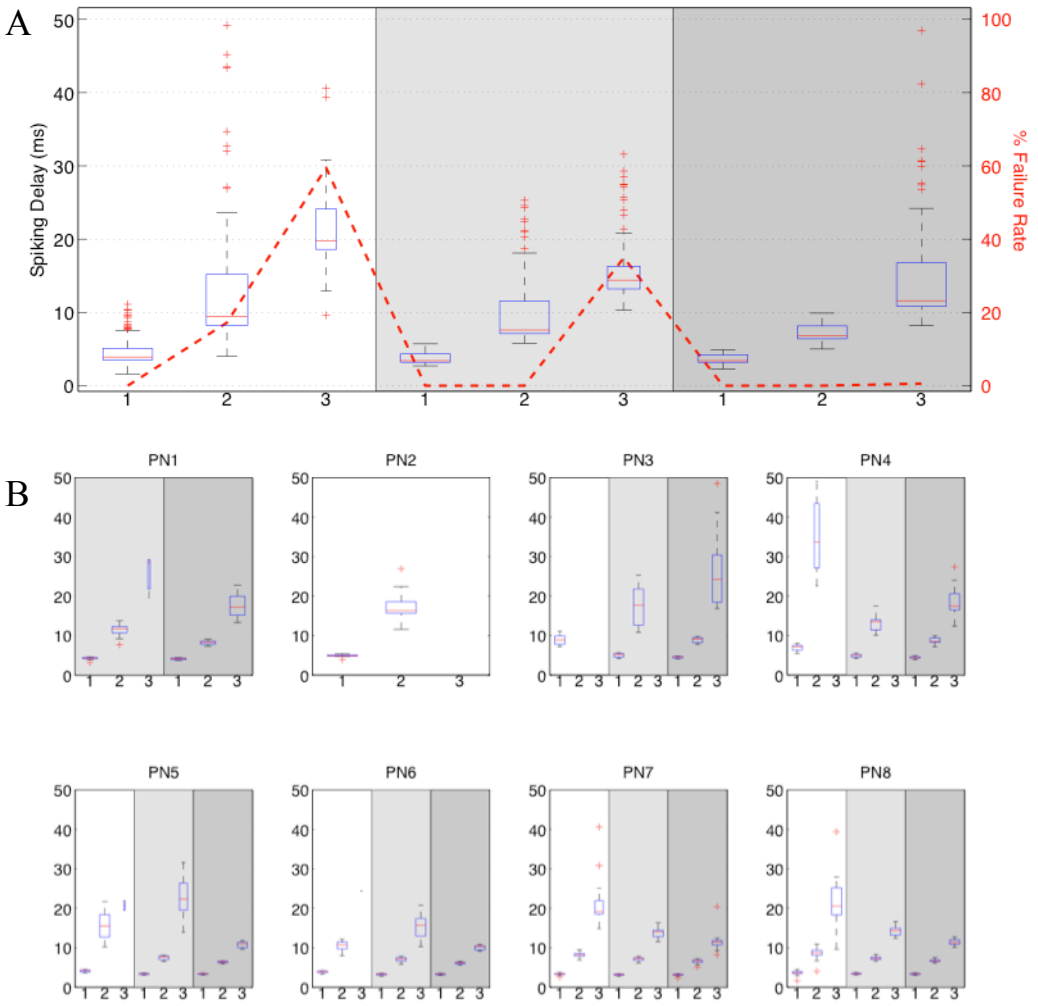

Figure 4.7 PN spiking latency reduces with stronger stimulation. **(A)** Boxplot of spiking latency for 1st, 2nd, and 3rd spikes for 1ms stimulation (white background), 2ms stimulation (light gray) and 5ms (dark gray). Overlaid dashed red line shows spike failure rate for each condition. **(B)** Same as A, but for all the individual cells (shading signifies stimulus duration). Note that the first two cells were not tested at all stimulation conditions. In all boxplots, the width of the box corresponds to the number of spikes it represents.

For this purpose we calculated the mean KC response to 1ms, 2ms and 5ms stimulation and binned them based of the number of connections they were observed to make (see table in Figure 4.8). We can now address the question of what induces a stronger post-synaptic response - adding a spike using the same claw or adding a spike through a different claw. We will first consider temporal integration. Increasing stimulation from 1 to 2ms (i.e. from one to two reliable input spikes) only increases the amplitude of postsynaptic response by 1mV (red dots in Figure 4.8A). In other words, adding a spike temporally increases the evoked responses by 1mV on average. Note however, that in neurons with three or more connections, adding a spike produced a significantly greater increase in the response than neurons with one or two connections ($p < 0.05$ Student t test). As with spiking responses and the magnitude of the evoked response, even at the low end of the stimulation regime three active connections are significantly different from just one or two. Overall, we found a similar increase in the post-synaptic response when we increased the stimulation from 2 to 5ms (i.e. from two to three reliable spikes; blue dots in Figure 4.8A).

A clear difference emerges when we consider spatial integration (Figure 4.8B). Increasing the number of connections from one to two does not have much effect on the magnitude of the response, regardless of the stimulation used (black curve). However, there is a large increase as the number of connections increases from two to three. The increase is to such a degree that the 5ms stimulus duration adds 3mV on average to the response amplitude (green curve). Again, as with spiking, evoked response amplitude, and temporal integration, the results change considerably with the addition of a third connection. Although this same increase is not observed as the number of connections increases from three to five (cyan curve), it is likely the result of the small number of instances where we observed five connections (we never observed four, a rare event we simply did not capture in our dataset). Juxtaposing the results for the temporal and the spatial integration, it is clear that spatial integration is much more efficient in the KC layer (Figure 4.8C).

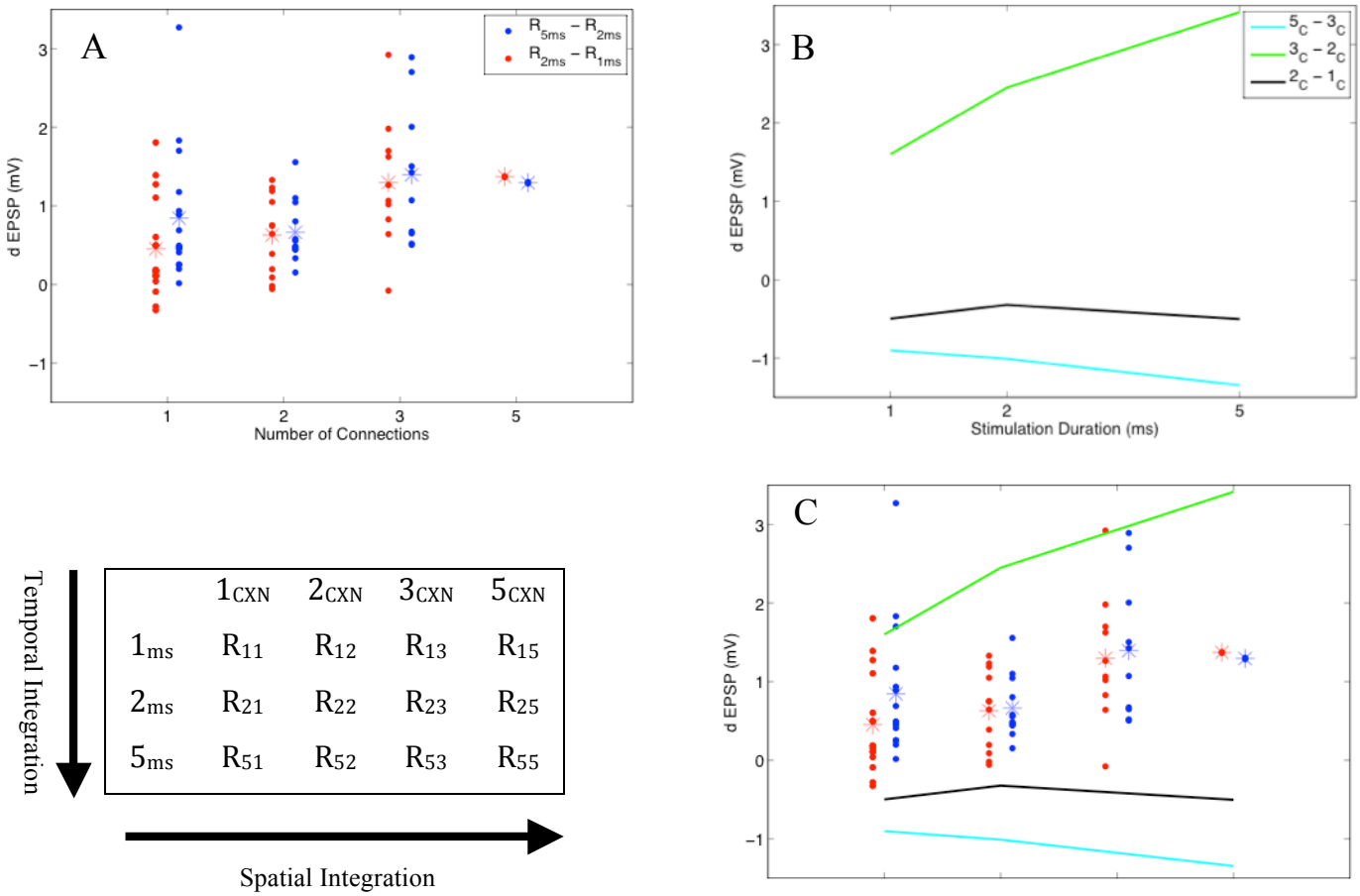

Figure 4.8 Spatial summation is more efficient than temporal summation in Kenyon cells. **(A)** Temporal integration. Increase in evoked response (mV) between 1ms and 2ms stimulation (red points) and between 2ms and 5ms (blue points). These increments are calculated for each connection number separately (1,2,3 or 5 connections). Dots represent the mean values from responses of individual cells while asterisks represent the mean for that number of connections. **(B)** Spatial integration. Increase in evoked response between cells with 2 and 1 connections (black), 3 and 2 connections (green), and 5 and 3 connections (cyan), calculated for each stimulation duration separately. **(C)** Figures A and B juxtaposed. Note the much stronger effect of adding an extra connection versus adding an extra spike.
Table in the left lower corner is meant for illustrative purposes. Figure A was generated by calculating $R_{2X} - R_{1X}$ (red) and $R_{5X} - R_{2X}$ (blue), and displaying it for each X (# connections) separately. Figure B was generated by calculating $R_{Y2} - R_{Y1}$ (black), $R_{Y3} - R_{Y2}$ (green), and $R_{Y5} - R_{Y3}$ (cyan), and displaying it for each Y (stimulation duration).

Though it is hard to draw conclusions about the integration properties of cells with five connections because of their small sample size, they do raise an interesting biological question – what is the probability of finding cells with five connections when one has only labeled 3 out of the possible 54 inputs? To address this question we counted the total number instances of each level of connectivity (Figure 9). It should be noted that the number of zero connections is partially deduced. As explained in the Methods section, although we have anatomical data from cells with zero connections, recordings from most of the non-responding cells were aborted and no image was acquired. Hence, their number of connections is deduced. Nevertheless, when compared to the number of cells that are expected to be found in a population (under the assumption of random connection probabilities) there is a striking difference. The expected number is calculated from a binomial distribution with $p = 3/54$ and N randomly sampled from our estimate of claws-per-cell from the previous experiment (see also Figure 3.1). Distributions are still incongruent even if we increase the connection probability to 10/54 and increase the number of claws for a cell to account for possibly missed claws.

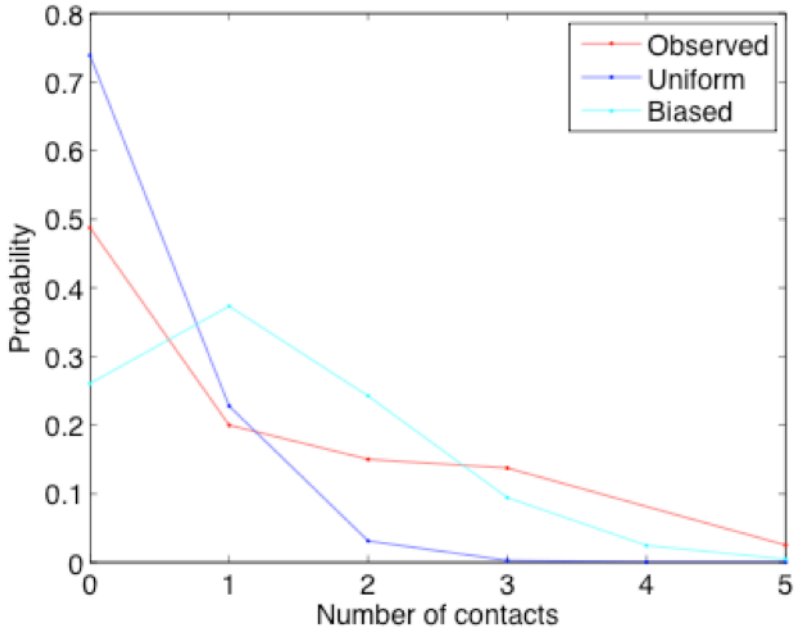

Figure 4.9 Distribution of number of synaptic contacts indicates biased connectivity between PNs and KCs. The observed number of connections is shown in comparison to the distribution expected if the probability of a PN-KC connection were uniform and random. All aborted recordings were added as zeros to the observed distribution. The distribution of connection numbers expected if connectivity were uniform and random was calculated using a binomial model with p=3/51 and the number of claws on a KC (N) drawn at random from the data in Figure 3.1. The biased distribution was calculated using a binomial model only in this case p=8/51 and the number of claws on each KC was uniformly increased by three to account for the possibility that we missed some claws. The distribution of observed synaptic contacts is considerably higher than both the uniform and the biased distributions.

The discrepancy between the observed and the expected curves corroborates our results from the previous experiment – sampling a particular PN channel increases the probability that a KC samples that channel again. It could be argued that we are looking at the connection probability of a very specific driver (Mz19) and it is different from the general population of PNs. Although the Mz19 driver line has been used in numerous experiments as a representative subset of the PN population (Ito et al. 1998; Tanaka et al. 2004; Berdnik et al. 2006; Jefferis et al. 2007; Lin et al. 2007; Tanaka et al. 2008; Okada et al. 2009; Kremer et al. 2010), we acknowledge that using this line might bias our results.

4.5 Discussion

In this chapter we have used ChR2 to drive a subset of PNs and recorded responses in individual KCs. We were able to recover anatomical connectivity between the recorded KC and stimulated PNs using a combination of genetic labels and intracellular dye-fills. This allowed us to conclude that having three active connections results in more reliable spiking (Figure 4.6A), stronger evoked responses (Figure 4.6F), and more efficient integration (Figure 4.8). Since it was also possible to induce firing in neurons with fewer than three connections, we believe that there is a great variability in the strength of individual KC connections. Possible reasons for this variability include both the variable anatomical structures we have detected (Figure 4.5) and the variability in the size of individual dendritic claws.

By comparing responses to the shortest stimulation duration, we were able to conclude that KCs are more efficient spatial integrators than temporal integrators. In other words, a KC responds more strongly if the additional input it gets comes from a different claw and not from an already active claw. This statement does not necessarily imply that KCs function as coincidence detectors. Though one possible model for KCs' sparse responses identifies them as coincidence detectors, our

data shows they can be driven to spike with just a single active input. The lower efficiency of temporal integration can be attributed, at least in part, to the nature of the PN to KC connections. From the anatomy of this unique connection it seems probable that the PN to KC connection is a depressing synapse, with a high probability of release but a depreciating response magnitude over time. This hypothesis is bolstered by a recent study that reported T-bar synapses in the PN boutons (Butcher et al. 2012). This type of synapse in flies have been shown to be exactly that - a depressing synapse with a high probability of release (Kittel et al. 2006). Therefore, the weaker efficiency of temporal integration could be a simple result of this depression, and not necessarily a result of a brief integration window, as in the locust (Jortner et al. 2007).

Comparing the observed number of connections with the number expected by chance, we have found that the connectivity pattern seems to be biased. This corroborates our finding from the imaging experiment, where individual claws from the same cell showed a high degree of correlation. Though the previous experiment had certain caveats associated with analyzing the degree of correlations between claws, the independent evidence presented here supports our suggestion that connections between PNs and KCs are biased. It is interesting to note that variable but non-random connections were recently found in *Drosophila's* olfactory circuit in the connectivity patterns of specific LNs in the antennal lobe (Chou et al. 2010).

Finally, we have also found that a single dendritic claw can form multiple connections with PN boutons (Figure 4.5D-F). The example shown in Figure 4.5F makes the finding even more surprising – it is not only that the claw contacts more then one bouton, but the second bouton is from a different PN type. This, in turn, transforms the single complex claw into an integration unit, though the properties of integration at that level have not been addressed in this study. While it could be claimed that a complex claw is actually several independent claws, it is obvious that integration within a complex claw is different from integration within claws. Since there is no thin neurite between the different parts of a complex claw, it seems likely that compartmentalization is weaker, if not completely absent.

5 Conclusions and Perspectives

5.1 Summary

How does the fly identify an odor? Since even monomolecular odorants activate multiple ORs, it is clear that integration across input channels is necessary. The first synapse in the olfactory circuit establishes the odor channels. ORNs expressing the same receptor converge to form synapses with a homotypic group of PNs. This convergent connectivity increases the signal to noise ratio, and lowers the odor detection threshold. Internal computations within the antennal lobe decorrelate the inputs, and increase their dynamic range, further establishing the independence of different glomerular channels. We have shown that the next synapse, between PNs and KCs, is where integration across channels occurs. By imaging odor responses in the dendritic claws of individual KCs, we were able to characterize the tuning curves of individual claws, and show that KCs receive inputs from different PN channels. By performing whole-cell recordings in KCs while controlling the spiking input from a small population of PNs, we established how much activity is needed to drive a KC to spike. We also characterized integration dynamics in the KC layer and showed that a KC integrates more efficiently across claws than within a claw. Analyzing the number of synaptic contacts we found between the PN subset and the individual KCs corroborates our conclusion from the correlations between claw tuning curves: KCs sample PN boutons in a biased manner.

5.2 Connectivity in the Mushroom Bodies

The biased connectivity we see in both number of connections and tuning curve correlations raise questions concerning the rules governing connectivity in the olfactory circuit of *Drosophila*. If the KC layer is indeed where odor objects are formed, it should be designed to represent as many

distinct odors as possible, and with the least probability of overlap. To exploit the KC coding space efficiently, an underlying principle needs to guide the PN to KC synapses. In what follows we will discuss what are the possible rules that guide this connection, and do they change throughout the life of the organism.

One answer to the connectivity problem, which is especially appealing in insects, is that connections are hard-wired. Indeed, several studies have shown that connections can form stereotypically even without active input. PNs form stereotypic projections in the lateral horn even before ORs are expressed (Marin et al. 2002), and both PNs and ORNs project to their corresponding glomeruli even when their cognate partners are inactive (Dobritsa et al. 2003; Berdnik et al. 2006). It is therefore acknowledged that development of the first two layers of olfactory system in *Drosophila* does not rely on evoked activity or OR expression, and is fairly hard-wired (sachse 2007 neuron).

Nonetheless, it has been shown that this extreme version of hard-wired specificity is not conveyed to the KC layer (Murthy et al. 2008). Even within the first two layers, LNs in the antennal lobe require activity for proper development (Chou et al. 2010). Additionally, it is clear that the olfactory system also exhibits a certain level of plasticity. For example, even highly stereotyped sub-circuits, like the CO_2 circuit, show changes in size and response magnitude in PNs and ORNs when flies are raised in conditions with constant CO_2 exposure (Sachse et al. 2007; Iyengar et al. 2010). Although plasticity in the mushroom bodies has not been measured directly, several morphological studies have shown environmental effects on calyx size (Technau 1984; Heisenberg et al. 1995). A more recent study has silenced a subset of PNs and found a size increase in the corresponding boutons and their matching KC claws (Kremer et al. 2010). Therefore, hard-wiring is probably only the solution for the first 2 layers (due to the small number of different inputs), and only during development.

Another possibility for guiding connectivity is complete randomness. By forming random branches in the calyx, the KC population can ensure an unbiased representation of the afferent inputs. However, anatomical evidence suggests this is not the case. Numerous studies have shown that PN

and KC projections in the calyx are non-random (Marin et al. 2002; Zhu et al. 2003; Tanaka et al. 2004; Lin et al. 2007); and to a lesser extent (Jefferis et al. 2007). Since PNs project with a certain spatial bias, a single KC would have to correct for this inherent bias to maintain an unbiased sampling. Additionally, random connectivity would not be helpful in the context of experience-based plasticity that likely occurs in the mushroom bodies.

Another possible connectivity rule is Hebbian wiring. According to this regime, Kenyon cells would preferentially connect to PNs with similar firing properties. Such a wiring scheme can ensure that KCs do not sample combinations of input that are rarely or never co-active. Even if we consider only half of the PN channels to be completely independent and even if we treat the channels as binary, this still leaves the encoding capacity of the system at 2^{25}. Since there are far fewer KCs, it would clearly be preferable to choose behaviorally/ethologically relevant combinations of input and not all the possible ones. Additionally, a Hebbian wiring scheme could contribute to concentration invariance of KC responses to odors. It has been shown that insects KCs display a significant degree of concentration invariance (Stopfer et al. 2003; Honegger et al. 2011). Examining responses of sensory neurons to increasing concentrations has shown that responses become less sparse, usually by recruiting more and more glomeruli as the concentration increases (Wang et al. 2003), see also Figure 5.1A). Naturally, this increases the correlation between PN activity patterns in the PN population. A KC that detects these correlations and wires to the relevant PNs could show considerable concentration invariance in its odor responses, with each additional channel increasing the certainty of the response. Using Figure 5.1 as an example, we can generate a KC that will respond invariably to odor 2. First, it will connect strongly with glomerulus 5, so as to guarantee a response to a low concentration. Next it will form slightly weaker connections to glomeruli 2 and 10, and an even weaker connection with glomerulus 4. As concentration increases, all the inputs still signal the same odor only with greater certainty. If this wiring scheme is utilized in the mushroom bodies it might explain the connectivity bias we see in our data.

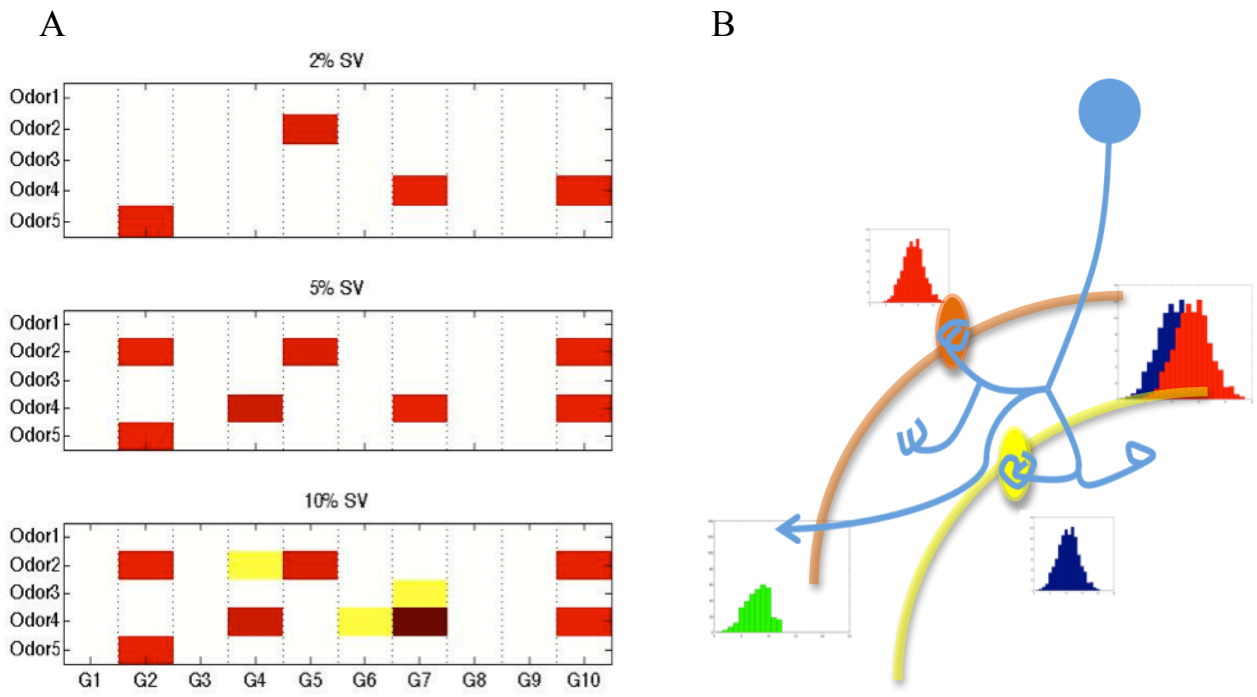

Figure 5.1 Possible scenarios for a single claw to induce spiking. **(A)** Adapted from Wang 2003 Cell (Figure 3). Increasing odor concentration recruits more glomeruli, but does not change the identity of the glomeruli that responded to low concentration. Therefore, to generate concentration invariance for Odor 2 for example, a KC might connect with glomeruli 2, 4, 5, and 10, with the strongest weight on glomerulus 5 (follow by 2 and 10, and weakest on 4). SV – saturated vapor **(B)** Receiving input from excitatory and inhibitory PNs with similar tuning might ensure that a KCs odor tuning is decorrelated from that of its inputs. In this example the yellow bouton is excitatory, while the orange bouton is inhibitory (corresponding tuning curves are shown adjacent to each bouton). The neuron's output is therefore the subtraction of the 2 tuning curves, which can further be thresholded. In our experiment, we may have stimulated just the excitatory bouton, which under natural conditions will never occur.

The last option for a wiring scheme we shall discuss is anti-Hebbian. Under this regime a KC will preferentially contact anti-correlated inputs. An advantage of using such a scheme could be a strong decorrelation of input, which will ensure KCs respond to rare and significant events (Barlow and Földiák 1989). Naturally, the system has to be tuned for combinations of inputs that still occur, so a balance has to be struck between rare events that are meaningful (detecting the scent of a rotten banana), and rare events that are meaningless (combinations of active glomeruli that are never encountered). However, the anti-Hebbian framework is usually considered on a shorter timescale. Use of this rule to regulate dendritic weights allows for the cancellation of predicted features in the inputs, and the accentuation of novelty (Roberts and Leen 2010). This trait serves a circuit mainly in adapting to the recent stimulus history, and not when forming substantial connections such as KC claws.

Because decorrelation of inputs would be a useful feature for the mushroom bodies, we shall now consider an alternative for achieving it without the use of anti-Hebbian plasticity. If a single KC integrates both active and inactive inputs, decorrelation can still be achieved using simple Hebbian wiring. Simply put, integration of inactive inputs means that the inactive channel also conveys information to the KC (see for example Osborne et al. 2008; Schneidman et al. 2011). If we imagine two correlated PN channels, one excitatory and one inhibitory, a KC that integrates over both of them would exhibit tuning that was highly decorrelated from the inputs (Figure 5.1B). Such a KC will only respond to odors at the periphery of the excitatory tuning curve, effectively decorrelating highly co-active inputs. Inhibitory PN inputs can either be direct - through GABAergic PNs (Jefferis et al. 2007; Okada et al. 2009), or indirect - through inverting the sign of the synaptic contribution of a dendritic claw. The latter can be accomplished by the pre-synaptic sites on the claw stems, which most likely activate GABAergic extrinsic neuron (Christiansen et al. 2011; Butcher et al. 2012).

To evaluate which of these different connectivity schemes is in play in the mushroom bodies, it will first be necessary to prove that there is plasticity at the KC layer. We believe plasticity to be a highly likely at this layer, since it has already been shown that certain LNs wire variably between individuals (Chou et al. 2010). In future experiments, we will raise flies in different odorized

environments: one odorized with odor A only, one with odor B and one with their combination. By imaging the responses of the KC population we hope to see if KCs have changed their response properties. Hebbian plasticity predicts that in flies reared in the third environment (combination) we will find more cells that respond specifically to the combination but not to the components. If we do see changes at this layer, we will use the ChR-based PN stimulation approach described in Chapter 4 to dissect the phenomenon even further. Studies have already shown that the *Drosophila* olfactory circuit displays a critical period (Sachse et al. 2007). Assuming that we find plasticity in the mushroom bodies, it would be interesting to stimulate a small subset of PNs during development using ChR2 (either larval stage or just post eclosion) and repeat the experiment that was performed in Chapter 4. This could potentially reveal a critical period for plasticity, and the effects it has on KC response properties. Will repeated stimulation of a PN subset induce more connections to a KC? Will individual connections evoke stronger responses or will they be suppressed? And will more or fewer connections be required to evoke a somatic response using the same stimulation regime?

5.3 The Sound of a Single Claw Spiking

Although the majority of our evidence indicates that KCs should be regarded as integrators, we have seen several examples where a single claw-bouton synaptic contact is capable of driving spiking in the connected KC. Does this mean that KCs are not integrators, and that they can simply be activated by any one of their inputs? In this light, it is useful to consider the integration properties we have already discussed above (Section 5.2). The first property that might provide a partial explanation for KC firing in response to activation of a single claw is concentration invariance. A KC could generate concentration invariant responses to the same odor by contacting all the PN channels that are successively recruited as concentration increases (Figure 5.1A). For the odor to be detected at the lowest concentration, the active channel should induce a response (glomerulus 5 for odor 2 in our example), and should therefore have a relatively large synaptic weight. If, by chance, we have

activated a PN that represents the lowest concentration of a particular odor, and recorded from its cognate KC, we should not be surprised to see a response.

An alternative explanation stems from the "synergy from silence" mechanism (Schneidman et al. 2011), which was discussed as an alternative for input decorrelation (section 5.2). As mentioned, inhibitory PN channels can result from GABAergic PNs or local inhibitory circuits inverting the contribution of an excitatory PN. PNs project form the antennal lobe in four main tracts, only one of which sends all its axons through the mushroom body calyx. These PNs are mainly excitatory (Okada et al. 2009). Nevertheless, some inhibitory PNs are found in this tract (Okada et al. 2009), and other inhibitory tracts have recently been found to project weakly into the calyx (Tanaka et al. 2008). It is possible that KCs still utilize the Hebbian scheme to connect to PNs with similar odor responses. If our hypothesis is correct and KCs integrate both excitatory and inhibitory PN channels (or if KCs simply invert the contribution of an excitatory PN), this will effectively induce decorrelation between the inputs. Under these conditions artificially stimulating only the excitatory channel without its inhibitory counter-point would drive the KC into an imbalance and induce spiking.

A simpler explanation for the potency of an individual claw might be found from a comparison to the PCx (the mammalian equivalent of mushroom bodies). Dissecting excitatory drive to the olfactory cortex has shown that the main drive is from intra-cortical connections and not mitral cells (Poo and Isaacson 2011). In our experiments we have also seen both functional and anatomical evidence suggesting strong connections between KCs. Several cells in the imaging experiment have displayed unusual somatic structures that seemed to envelop another soma. During our KC whole-cell recordings, we frequently (about 1 in 10) observed an adjacent soma filled with dye, indicating the existence of gap junctions between these cells. And several cells have also shown responses that suggest the presence of strong recurrent activity, which in some cases forced us to increase the interval between photostimulation events by several seconds. Though this does not establish the main drive to the KCs as intra-calycal, it does argue for strong lateral connections. In insects, these connections have been suggested to play a role in inhibitory gain control (Papadopoulou et al. 2011).

Since we have removed the antennae in these experiments, the global input to the system is low. As a result, these mechanisms will ensure that the gain is relatively high, which could account for the cases where even a single input is sufficient to induce spiking. Although these suggestions are speculative, it would be interesting to pursue this path further. The first step towards such as inquiry would be to repeat the experiment with the antennae intact. Though it would be harder to identify the evoked responses, it is possible that baseline activity (that is almost absent under our current experimental conditions) plays a crucial role in shaping KC responses.

5.4 The Quest for Meaning

As the introduction to my thesis implied, my main interest lies not in what the animal senses but in what it perceives. This might be a small semantic change on paper, but experimentally it involves completely different frameworks. Though I cannot claim to have found meaning in the fly's brain just yet, I believe that I took a step in that direction. Perhaps it is not so much a search for meaning but a long and arduous quest that, again as implied, might require several sequels of a "next generation" series.

Pursuing such a quest in the fly as a model organism seems ideal. On the one hand, it is simple enough. It has a well-characterized olfactory system, with major parts of the anatomy and the functionality of the different layers ironed out. We know it has only 54 different input channels, we know some of their response properties, and we know how they connect. We also know that a fly neuron is simpler than a mammalian neuron. It is impossible to follow all the inputs of a single pyramidal cell, but the major olfactory inputs to a KC are less than ten. On the other hand, the fly is complex enough. It is a sophisticated organism that is capable of learning in several different assays. It displays complex, yet stereotypical behaviors (such as courtship and aggression) that are modulated by the environment and its internal conditions.

From what we currently know about the olfactory system in *Drosophila*, it seems that the KCs are a significant step in odor processing. Responses are much less sparse both before and after the mushroom bodies. Since the distance between the KCs and the actual motor output cannot be more than a few synapses away, it seems likely that meaning in the fly's olfactory system will be found in our lifetime.

6 List of Abbreviations

ChR2	Channelrhodopsin 2
F	Fluorescence
KC	Kenyon Cell
LN	Local Inter-neuron
MARCM	Mosaic Analysis with a Repressible Cell Marker
OR	Olfactory Receptor
ORN	Olfactory Receptor Neuron
PCx	Piriform Cortex
PID	Photoionization Detector
PN	Projection Neuron
RGC	Retinal Ganglion Cell
ROI	Region Of Interest
TTX	Tetrodotoxin
YFP	Yellow Fluorescent Protein
ΔG/R	Delta Green Fluorescence Over Red Fluorescence

7 List of Figures

8 References

Abramoff, M.D., Magalhaes, P.J., and Ram, S.J. 2004. Image processing with ImageJ. *Biophotonics International* **11**(7): 36-42.

Ache, B.W. and Young, J.M. 2005. Olfaction: diverse species, conserved principles. *Neuron* **48**(3): 417-430.

Attneave, F. 1954. Some informational aspects of visual perception. *Psychol Rev* **61**(3): 183-193.

Bargmann, C.I. 2006. Comparative chemosensation from receptors to ecology. *Nature* **444**(7117): 295-301.

Barlow, H. 1953. Summation and inhibition in the frog's retina. *J Physiol (Lond)* **119**(1): 69-88.

-. 1985a. Cerebral cortex as model builder. in *Models of the visual cortex* (ed. D.a.D. Rose, V. G.), pp. 37-46. Wiley, New York.

-. 2001. Redundancy reduction revisited. *Network (Bristol, England)* **12**(3): 241-253.

Barlow, H.B. 1972. Single units and sensation: A neuron doctrine for perceptual psychology? *Perception* **1**: 371-394.

-. 1985b. The role of single neurons in the psychology of perception. *Q J Exp Psychology* **37A**: 121-145.

Barlow, H.B. and Földiák, P. 1989. Adaptation and decorrelation in the cortex. in *The Computing Neuron* (ed. R. Durbin, C. Miall, and G. Mitchison), pp. 54-72. Addison-Wesley, Wokingham, England.

Berdnik, D., Chihara, T., Couto, A., and Luo, L. 2006. Wiring stability of the adult Drosophila olfactory circuit after lesion. *Journal of Neuroscience* **26**(13): 3367-3376.

Bhandawat, V., Olsen, S.R., Gouwens, N., and Schlief, M. 2007. Sensory processing in the Drosophila antennal lobe increases reliability and separability of …. *Nature Neuroscience*.

Brandstaetter, A.S. and Kleineidam, C.J. 2011. Distributed representation of social odors indicates parallel processing in the antennal lobe of ants. *J Neurophysiol* **106**(5): 2437-2449.

Butcher, N.J., Friedrich, A.B., Lu, Z., Tanimoto, H., and Meinertzhagen, I.A. 2012. Different classes of input and output neurons reveal new features in microglomeruli of the adult Drosophila mushroom body calyx. *J Comp Neurol*: n/a-n/a.

Chou, Y.-H., Spletter, M.L., Yaksi, E., Leong, J.C.S., Wilson, R.I., and Luo, L. 2010. Diversity and wiring variability of olfactory local interneurons in the Drosophila antennal lobe. *Nature Neuroscience* **13**(4): 439-449.

Christiansen, F., Zube, C., Andlauer, T.F.M., Wichmann, C., Fouquet, W., Owald, D., Mertel, S., Leiss, F., Tavosanis, G., Farca Luna, A.J. et al. 2011. Presynapses in Kenyon Cell Dendrites in the Mushroom Body Calyx of Drosophila. *J Neurosci* **31**(26): 9696-9707.

Connolly, J.B., Roberts, I.J., Armstrong, J.D., Kaiser, K., Forte, M., Tully, T., and O'Kane, C.J. 1996. Associative learning disrupted by impaired Gs signaling in Drosophila mushroom bodies. *Science* **274**(5295): 2104-2107.

Davison, I.G. and Ehlers, M.D. 2011. Neural circuit mechanisms for pattern detection and feature combination in olfactory cortex. *Neuron* **70**(1): 82-94.

de Belle, J.S. and Heisenberg, M. 1994. Associative odor learning in Drosophila abolished by chemical ablation of mushroom bodies. *Science* **263**(5147): 692-695.

de Vries, S.E.J. and Clandinin, T.R. 2012. Loom-sensitive neurons link computation to action in the Drosophila visual system. *Curr Biol* **22**(5): 353-362.

Dobritsa, A.A., van der Goes van Naters, W., Warr, C.G., Steinbrecht, R.A., and Carlson, J.R. 2003. Integrating the molecular and cellular basis of odor coding in the Drosophila antenna. *Neuron* **37**(5): 827-841.

Dubnau, J., Grady, L., Kitamoto, T., and Tully, T. 2001. Disruption of neurotransmission in Drosophila mushroom body blocks retrieval but not acquisition of memory. *Nature* **411**(6836): 476-480.

Fantana, A.L., Soucy, E.R., and Meister, M. 2008. Rat olfactory bulb mitral cells receive sparse glomerular inputs. *Neuron* **59**(5): 802-814.

Fishilevich, E. and Vosshall, L.B. 2005. Genetic and functional subdivision of the Drosophila antennal lobe. *Curr Biol* **15**(17): 1548-1553.

Galizia, G. and Rössler, W. 2010. Parallel Olfactory Systems in Insects: Anatomy and Function. *Annu Rev Entomol* **55**(1): 399-420.

Ghosh, S., Larson, S.D., Hefzi, H., Marnoy, Z., Cutforth, T., Dokka, K., and Baldwin, K.K. 2011. Sensory maps in the olfactory cortex defined by long-range viral tracing of single neurons. *Nature* **472**(7342): 217-220.

Gollisch, T. and Meister, M. 2010. Eye smarter than scientists believed: neural computations in circuits of the retina. *Neuron* **65**(2): 150-164.

Gordon, M.D. and Scott, K. 2009. Motor control in a Drosophila taste circuit. *Neuron* **61**(3): 373-384.

Gottfried, J.A. 2010. Central mechanisms of odour object perception. *Nat Rev Neurosci* **11**(9): 628-641.

Gross, C.G., Rocha-Miranda, C.E., and Bender, D.B. 1972. Visual properties of neurons in inferotemporal cortex of the Macaque. *Journal of neurophysiology* **35**(1): 96-111.

Grossman, N., Nikolic, K., Toumazou, C., and Degenaar, P. 2011. Modeling study of the light stimulation of a neuron cell with channelrhodopsin-2 mutants. *IEEE Trans Biomed Eng* **58**(6): 1742-1751.

Guizar-Sicairos, M., Thurman, S.T., and Fienup, J.R. 2008. Efficient subpixel image registration algorithms. *Opt Lett* **33**(2): 156-158.

Gupta, N. and Stopfer, M. 2011. Insect olfactory coding beyond mushroom bodies: Structure and function of lateral horn neurons In *SFN*, Washington, D.C.

Hallem, E.A. and Carlson, J.R. 2006. Coding of odors by a receptor repertoire. *Cell* **125**(1): 143-160.

Hallem, E.A., Ho, M.G., and Carlson, J.R. 2004. The molecular basis of odor coding in the Drosophila antenna. *Cell* **117**(7): 965-979.

Hateren, J.H.v. and Schaaf, A.v.d. 1998. Independent component filters of natural images compared with simple cells in primary visual cortex. *Proceedings of the Royal Society B: Biological Sciences* **265**(1394): 359.

Heisenberg, M., Heusipp, M., and Wanke, C. 1995. Structural plasticity in the Drosophila brain. *J Neurosci* **15**(3 Pt 1): 1951-1960.
Honegger, K.S., Campbell, R.A.A., and Turner, G.C. 2011. Cellular-resolution population imaging reveals robust sparse coding in the Drosophila mushroom body. *J Neurosci* **31**(33): 11772-11785.
Hu, A., Zhang, W., and Wang, Z. 2010. Functional feedback from mushroom bodies to antennal lobes in the Drosophila olfactory pathway. *Proc Natl Acad Sci USA*.
Hubel, D.H. and Wiesel, T.N. 1962. Receptive fields, binocular interaction and functional architecture in the cat's visual cortex. *J Physiol (Lond)* **160**: 106-154.
Hwang, R.Y., Zhong, L., Xu, Y., Johnson, T., Zhang, F., Deisseroth, K., and Tracey, W.D. 2007. Nociceptive neurons protect Drosophila larvae from parasitoid wasps. *Curr Biol* **17**(24): 2105-2116.
Ito, K., Suzuki, K., Estes, P., Ramaswami, M., Yamamoto, D., and Strausfeld, N.J. 1998. The organization of extrinsic neurons and their implications in the functional roles of the mushroom bodies in Drosophila melanogaster Meigen. *Learn Mem* **5**(1-2): 52-77.
Iyengar, A., Chakraborty, T.S., Goswami, S.P., Wu, C.-F., and Siddiqi, O. 2010. Post-eclosion odor experience modifies olfactory receptor neuron coding in Drosophila. *Proceedings of the National Academy of Sciences* **107**(21): 9855-9860.
Jefferis, G.S.X.E., Potter, C.J., Chan, A.M., Marin, E.C., Rohlfing, T., Maurer, C.R., and Luo, L. 2007. Comprehensive maps of Drosophila higher olfactory centers: spatially segregated fruit and pheromone representation. *Cell* **128**(6): 1187-1203.
Jefferis, G.S.X.E., Vyas, R.M., Berdnik, D., Ramaekers, A., Stocker, R.F., Tanaka, N.K., Ito, K., and Luo, L. 2004. Developmental origin of wiring specificity in the olfactory system of Drosophila. *Development* **131**(1): 117-130.
Jia, H., Rochefort, N.L., Chen, X., and Konnerth, A. 2010. Dendritic organization of sensory input to cortical neurons in vivo. *Nature* **464**(7293): 1307-1312.
Jortner, R.A., Farivar, S.S., and Laurent, G. 2007. A simple connectivity scheme for sparse coding in an olfactory system. *J Neurosci* **27**(7): 1659-1669.
Kadohisa, M. and Wilson, D.A. 2006. Separate encoding of identity and similarity of complex familiar odors in piriform cortex. *Proc Natl Acad Sci USA* **103**(41): 15206-15211.
Kazama, H. and Wilson, R.I. 2008. Homeostatic matching and nonlinear amplification at identified central synapses. *Neuron* **58**(3): 401-413.
-. 2009. Origins of correlated activity in an olfactory circuit. *Nature Neuroscience*.
Kittel, R.J., Wichmann, C., Rasse, T.M., Fouquet, W., Schmidt, M., Schmid, A., Wagh, D.A., Pawlu, C., Kellner, R.R., Willig, K.I. et al. 2006. Bruchpilot promotes active zone assembly, Ca2+ channel clustering, and vesicle release. *Science* **312**(5776): 1051-1054.
Krashes, M.J., Keene, A.C., Leung, B., Armstrong, J.D., and Waddell, S. 2007. Sequential use of mushroom body neuron subsets during drosophila odor memory processing. *Neuron* **53**(1): 103-115.
Kremer, M.C., Christiansen, F., Leiss, F., Paehler, M., Knapek, S., Andlauer, T.F.M., Förstner, F., Kloppenburg, P., Sigrist, S.J., and Tavosanis, G. 2010. Structural Long-Term Changes at Mushroom Body Input Synapses. *Curr Biol*.

Laissue, P.P. and Vosshall, L.B. 2008. The olfactory sensory map in Drosophila. *Brain Development in Drosophila Melanogaster*: 102-114.
Lee, T., Lee, A., and Luo, L. 1999. Development of the Drosophila mushroom bodies: sequential generation of three distinct types of neurons from a neuroblast. *Development* **126**(18): 4065-4076.
Leiss, F., Groh, C., Butcher, N., Meinertzhagen, I.A., and Tavosanis, G. 2009. Synaptic organization in the adult Drosophila mushroom body calyx. *J Comp Neurol* **517**(6): 808-824.
Li, W., Howard, J.D., Parrish, T.B., and Gottfried, J.A. 2008. Aversive learning enhances perceptual and cortical discrimination of indiscriminable odor cues. *Science* **319**(5871): 1842-1845.
Lin, H.-H., Lai, J.S.-Y., Chin, A.-L., Chen, Y.-C., and Chiang, A.-S. 2007. A map of olfactory representation in the Drosophila mushroom body. *Cell* **128**(6): 1205-1217.
Liu, X. and Davis, R.L. 2008. The GABAergic anterior paired lateral neuron suppresses and is suppressed by olfactory learning. *Nature Neuroscience*.
Luo, S.X., Axel, R., and Abbott, L.F. 2010. Generating sparse and selective third-order responses in the olfactory system of the fly. *Proc Natl Acad Sci USA*.
Marin, E.C., Jefferis, G.S.X.E., Komiyama, T., Zhu, H., and Luo, L. 2002. Representation of the glomerular olfactory map in the Drosophila brain. *Cell* **109**(2): 243-255.
MathWorks. 2010. MATLAB. In. The MathWorks Inc., Natick, Massachusetts.
McGrath, P.T., Xu, Y., Ailion, M., Garrison, J.L., Butcher, R.A., and Bargmann, C.I. 2011. Parallel evolution of domesticated Caenorhabditis species targets pheromone receptor genes. *Nature* **477**(7364): 321-325.
Mitsui, S., Igarashi, K.M., Mori, K., and Yoshihara, Y. 2011. Genetic visualization of the secondary olfactory pathway in Tbx21 transgenic mice. *Neural Syst Circuits* **1**(1): 5.
Miyamichi, K., Amat, F., Moussavi, F., Wang, C., Wickersham, I., Wall, N.R., Taniguchi, H., Tasic, B., Huang, Z.J., He, Z. et al. 2011. Cortical representations of olfactory input by trans-synaptic tracing. *Nature* **472**(7342): 191-196.
Murthy, M., Fiete, I., and Laurent, G. 2008. Testing odor response stereotypy in the Drosophila mushroom body. *Neuron* **59**(6): 1009-1023.
Okada, R., Awasaki, T., and Ito, K. 2009. Gamma-aminobutyric acid (GABA)-mediated neural connections in the Drosophila antennal lobe. *J Comp Neurol* **514**(1): 74-91.
Olsen, S.R., Bhandawat, V., and Wilson, R.I. 2007. Excitatory interactions between olfactory processing channels in the Drosophila antennal lobe. *Neuron* **54**(1): 89-103.
-. 2010. Divisive normalization in olfactory population codes. *Neuron* **66**(2): 287-299.
Olsen, S.R. and Wilson, R.I. 2008. Lateral presynaptic inhibition mediates gain control in an olfactory circuit. *Nature*.
Osborne, L.C., Palmer, S.E., Lisberger, S.G., and Bialek, W. 2008. The neural basis for combinatorial coding in a cortical population response. *J Neurosci* **28**(50): 13522-13531.
Papadopoulou, M., Cassenaer, S., Nowotny, T., and Laurent, G. 2011. Normalization for sparse encoding of odors by a wide-field interneuron. *Science* **332**(6030): 721-725.

Perrett, D.I., Rolls, E.T., and Caan, W. 1982. Visual neurones responsive to faces in the monkey temporal cortex. *Exp Brain Res* **47**(3): 329-342.
Phillips, C.G., Zeki, S., and Barlow, H.B. 1984. Localization of function in the cerebral cortex. Past, present and future. *Brain* **107 (Pt 1)**: 327-361.
Poo, C. and Isaacson, J.S. 2011. A major role for intracortical circuits in the strength and tuning of odor-evoked excitation in olfactory cortex. *Neuron* **72**(1): 41-48.
Pressnitzer, D., Suied, C., and Shamma, S.A. 2011. Auditory scene analysis: the sweet music of ambiguity. *Front Hum Neurosci* **5**: 158.
Roberts, P.D. and Leen, T.K. 2010. Anti-Hebbian Spike-Timing-Dependent Plasticity and Adaptive Sensory Processing. *Front Comput Neurosci* **4**: 1-11.
Rubin, B.D. and Katz, L.C. 2001. Spatial coding of enantiomers in the rat olfactory bulb. *Nature Neuroscience* **4**(4): 355-356.
Sachse, S., Rueckert, E., Keller, A., Okada, R., Tanaka, N.K., Ito, K., and Vosshall, L.B. 2007. Activity-dependent plasticity in an olfactory circuit. *Neuron* **56**(5): 838-850.
Sanes, J.R. and Zipursky, S.L. 2010. Design Principles of Insect and Vertebrate Visual Systems. *Neuron* **66**(1): 15-36.
Sato, K., Pellegrino, M., Nakagawa, T., Nakagawa, T., Vosshall, L.B., and Touhara, K. 2008. Insect olfactory receptors are heteromeric ligand-gated ion channels. *Nature* **452**(7190): 1002-1006.
Schneidman, E., Puchalla, J.L., Segev, R., Harris, R.A., Bialek, W., and Berry, M.J. 2011. Synergy from Silence in a Combinatorial Neural Code. *J Neurosci* **31**(44): 15732-15741.
Schwaerzel, M., Monastirioti, M., Scholz, H., Friggi-Grelin, F., Birman, S., and Heisenberg, M. 2003. Dopamine and octopamine differentiate between aversive and appetitive olfactory memories in Drosophila. *J Neurosci* **23**(33): 10495-10502.
Semmelhack, J.L. and Wang, J. 2009. Select Drosophila glomeruli mediate innate olfactory attraction and aversion. *Nature*.
Sherrington, C.S. 1923. *The Integrative Action of the Nervous System*. Ayer Co Pub.
Sosulski, D.L., Bloom, M.L., Cutforth, T., Axel, R., and Datta, S.R. 2011. Distinct representations of olfactory information in different cortical centres. *Nature*.
Stettler, D.D. and Axel, R. 2009. Representations of odor in the piriform cortex. *Neuron* **63**(6): 854-864.
Stopfer, M., Jayaraman, V., and Laurent, G. 2003. Intensity versus identity coding in an olfactory system. *Neuron* **39**(6): 991-1004.
Strausfeld, N.J. and Hildebrand, J.G. 1999. Olfactory systems: common design, uncommon origins? *Curr Opin Neurobiol* **9**(5): 634-639.
Strausfeld, N.J., Sinakevitch, I., and Vilinsky, I. 2003. The mushroom bodies of Drosophila melanogaster: an immunocytological and golgi study of Kenyon cell organization in the calyces and lobes. *Microsc Res Tech* **62**(2): 151-169.
Suh, G.S.B., Wong, A.M., Hergarden, A.C., Wang, J.W., Simon, A.F., Benzer, S., Axel, R., and Anderson, D.J. 2004. A single population of olfactory sensory neurons mediates an innate avoidance behaviour in Drosophila. *Nature* **431**(7010): 854-859.
Tanaka, N.K., Awasaki, T., Shimada, T., and Ito, K. 2004. Integration of chemosensory pathways in the Drosophila second-order olfactory centers. *Curr Biol* **14**(6): 449-457.

Tanaka, N.K., Tanimoto, H., and Ito, K. 2008. Neuronal assemblies of the Drosophila mushroom body. *J Comp Neurol* **508**(5): 711-755.
Technau, G.M. 1984. Fiber number in the mushroom bodies of adult Drosophila melanogaster depends on age, sex and experience. *J Neurogenet* **1**(2): 113-126.
Thum, A.S., Jenett, A., Ito, K., Heisenberg, M., and Tanimoto, H. 2007. Multiple memory traces for olfactory reward learning in Drosophila. *J Neurosci* **27**(41): 11132-11138.
Tian, L., Hires, S., Mao, T., Huber, D., Chiappe, M., Chalasani, S., Petreanu, L., Akerboom, J., McKinney, S., Schreiter, E. et al. 2009. Imaging neural activity in worms, flies and mice with improved GCaMP calcium indicators. *Nature Methods*.
Tsunozaki, M., Chalasani, S., and Bargmann, C.I. 2008. A Behavioral Switch: cGMP and PKC Signaling in Olfactory Neurons Reverses Odor Preference in C. …. *Neuron*.
Tully, T. and Quinn, W.G. 1985. Classical conditioning and retention in normal and mutant Drosophila melanogaster. *J Comp Physiol A Neuroethol Sens Neural Behav Physiol* **157**(2): 263-277.
Turner, G.C., Bazhenov, M., and Laurent, G. 2008. Olfactory representations by Drosophila mushroom body neurons. *J Neurophysiol* **99**(2): 734-746.
Uexkull, J.V. 1982. The theory of meaning. *Semiotica* **42**(1): 25-82.
Varga, Z., Jia, H., Sakmann, B., and Konnerth, A. 2011. Dendritic coding of multiple sensory inputs in single cortical neurons in vivo. *Proceedings of the National Academy of Sciences*: 1-6.
Vosshall, L.B., Wong, A.M., and Axel, R. 2000. An olfactory sensory map in the fly brain. *Cell* **102**(2): 147-159.
Wang, J.W., Wong, A.M., Flores, J., Vosshall, L.B., and Axel, R. 2003. Two-photon calcium imaging reveals an odor-evoked map of activity in the fly brain. *Cell* **112**(2): 271-282.
Wilson, R.I., Turner, G.C., and Laurent, G. 2004. Transformation of olfactory representations in the Drosophila antennal lobe. *Science* **303**(5656): 366-370.
Yusuyama, K., Meinertzhagen, I.A., and Schürmann, F.-W. 2002. Synaptic organization of the mushroom body calyx in Drosophila melanogaster. *J Comp Neurol* **445**(3): 211-226.
Zhu, S., Chiang, A.-S., and Lee, T. 2003. Development of the Drosophila mushroom bodies: elaboration, remodeling and spatial organization of dendrites in the calyx. *Development* **130**(12): 2603-2610.